

[Note to readers: this is from the book *Visual Practices Across the University*, edited by James Elkins (Munich: Wilhelm Fink Verlag, 2007). This book is available on Amazon.

This pdf was originally posted on the author's website, www.jameselkins.com, and other sites. Please send all comments to the author at jameselkins@fastmail.fm or via the website.]

10

Visual Representation of Speech and Sounds

Paul Fletcher and James Elkins

Spectrograms reveal the acoustic nature of sound in two dimensions. The horizontal axis records time. The dark spectrogram is the song of the canyon wren; it is a series of rapid rising notes. As the song goes on — really only four seconds — the little rising notes fall, and to a human ear the result is a falling melody. The green spectrogram is part of the lark sparrow's song. It is much more complex, and over the course of three seconds it makes many rhythmic and tonal changes. To an unaided human ear, it sounds like lovely chirping, but with the help of the sonogram it is possible to hear much more — the visual dissection helps the ear to discern things that would otherwise be too rapid to catch.

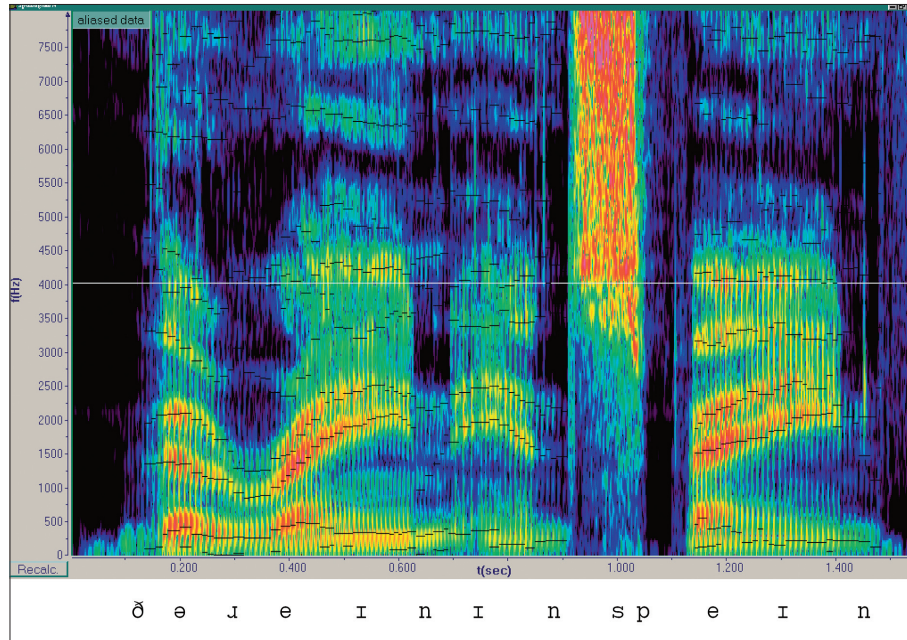
Bird sonograms are increasingly popular, and several software packages make them accessible to amateurs. The Bird sonograms at the beginning and the end of this Chapter were made using software called Raven and Amadeus; the former is used by professional ornithologists.

Human speech spectrograms

In the spectrogram on the next page, someone is saying “the rain in Spain”; it takes less than 1 1/2 seconds.

The second dimension of a spectrogram, after time, is frequency, in this case measured from 0 to 8000 cycles per second (cps, or Hertz). Frequency is labelled on the y axis. The human ear can detect frequencies from 15 Hz to 20,000 Hz, and the voice includes frequencies higher than those shown here.

The third dimension is intensity (loudness). Here color represents loudness: black corresponds to the lowest volume, and louder sounds move through violet, blue, yellow, and orange, to red.



The continuous acoustic signal

The acoustic signal is continuous. Because the linguistic representation that we are most familiar with is the written form, we tend to think that words have spaces between them. As you can see, this is not the case. There is some black on the spectrogram, which signals silence, but the most obvious instance comes within a word, when the “p” sound in “Spain” is being pronounced. This is because in producing this sound you close your lips very briefly (for less than one-tenth of a second) and no sound comes out.

Vowels

You will see concentrations of acoustic energy, some colored red, in the lower half of the frequency range, between 500 and 2000 Hz. These are characteristic of vowels, and each of the vowels has three obvious arc-shaped concentrations, called ‘formants’. It is the shape of these *formants*, their relationship to one another, and their duration, that enables us to identify different vowels.

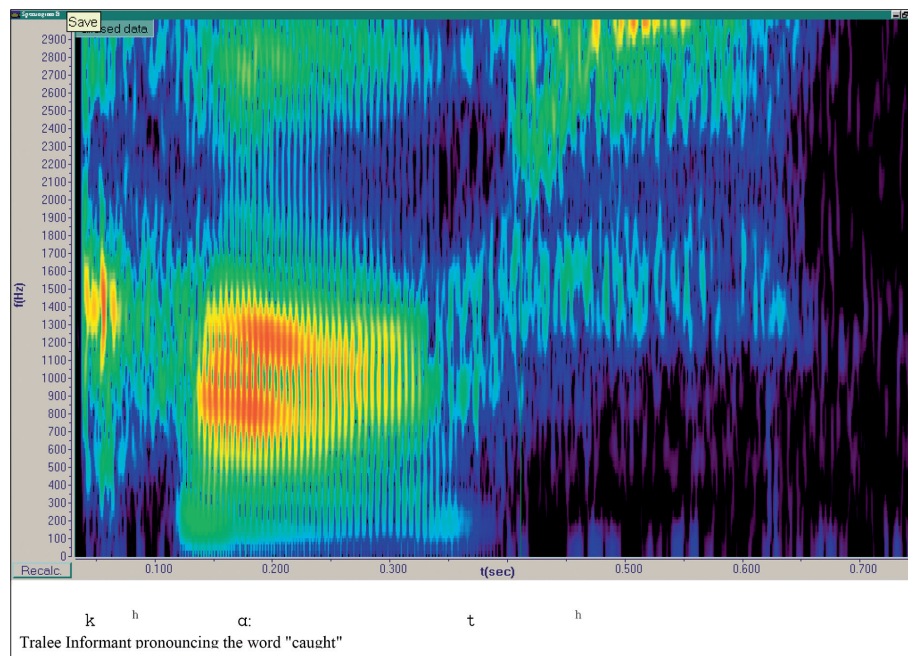
Formants are a little like harmonics in music, but not as predictable. They are resonance frequencies overlaid on the fundamental frequency by the structure of the vocal tract. We hear the vowels in “rain” and “Spain” as the same. In the spectrogram, their formants have the same shape, are in the same spatial orientation to one another, and are the same length. The individual sounds are identified

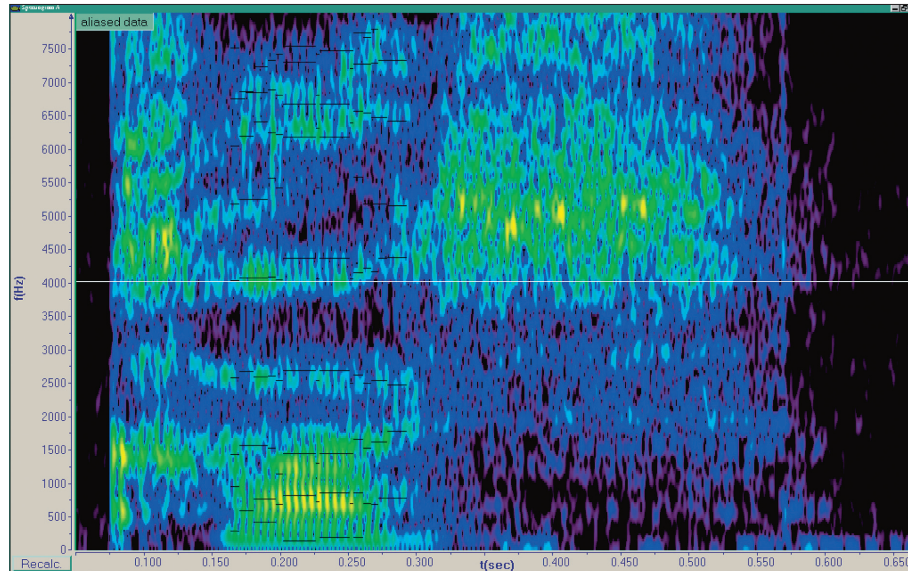
below the spectrogram using symbols from the International Phonetic Alphabet (IPA). This is used because English orthography can be misleading, especially as to the sounds of vowels.

Accents

The quality of vowels is very important in distinguishing accents of English. Here are two spectrograms comparing the word “caught” spoken by a native of Tralee in Ireland, and by a native of Bandon, both female and of similar ages. Once again IPA symbols under the spectrogram identifies the different sounds in the words. (This is a funny comparison to people in Ireland: Tralee is a tourist destination, and home of a popular beauty contest; Bandon, to put it politely, isn’t a tourist destination.)

Most noticeable is the difference in the length of the vowels. The Bandon vowel is shorter and sounds more like the vowel in “cot,” while the Tralee pronunciation is longer. The shape of the formants differs also. Most relevant to our identification of accentual differences are the first three formants. Formants higher up the range (easier to see in the Tralee vowel) are important in identifying individual differences between speakers.

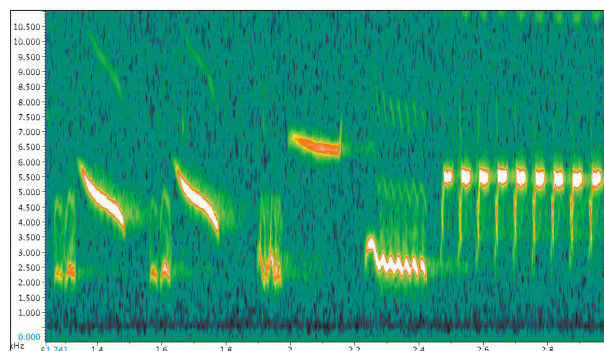




Individual speakers

Phonograms are common in the mass media when they are shown as “voice-prints”: ways of identifying individual speakers on audiotapes. Such differences are very subtle. The Bandon speaker’s voice looks “rougher”: the corrugations are glottal (laryngeal) pulses, possibly traits of that individual speaker.

Phoneticians distinguish between speaker verification and elimination (which is relatively easy) and speaker identification (which is prone to error). In the first cases one compares a spectrogram from speaker A with a previously stored spectrogram from speaker A, or another speaker. Speaker identification (the voiceprint case) is much trickier, and informed research would suggest that it cannot yet be done reliably.



Spectrograms as pictures

Spectrograms are a good example of one of the themes proposed in the Introduction: they look like naturalistic images, but they aren't. (There have already been several examples, in Chapters 1 and 6.) Somehow, their image-like configuration makes them more useful than they might be if their information were presented in tabular form (as in the Nagios software discussed in Chapter 7). Somehow, they help us to discern what we hear more accurately. Birdwatchers slow down spectrograms so they can pry apart the rapid changes in birdsong, and there are ways of exaggerating the vertical scale and the color schema. But even without those enhancements, the picturelike quality of the spectrograms lets them speak — or sing — more clearly.

For further reading

A. Hughes and P. Trudgill, *English Accents and Dialects* (London: Arnold, 1996); R. Kent and C. Read, *Acoustic Analysis of Speech*, second edition (Albany NY: Singular, 2002); P. Ladefoged, *Vowels and Consonants* (Oxford: Blackwell Publishers, 2001); David Rothenberg, *Why Birds Sing: A Journey Through the Mystery of Bird Song* (New York: Basic Books, 2005).



11

Matching Shades of Crowns

Francis Burke and Catherine Gorman

It may seem that teeth just range from sparkly white to tea-stain brown: that would be a simple change in hue, and a lowering of value. But in fact some teeth have a wide color range, and they also vary in chroma. (Color is best quantified according to its three dimensions: hue, for example blue, red, or green; the chroma, which is the intensity or saturation of color; and the value, the level of brightness of the color.)

The challenge for dentists is that the differences in the hue, value, and chroma of individual teeth are very subtle but crucial to providing the patient with a crown that matches perfectly. (Artists have it easy by comparison!)

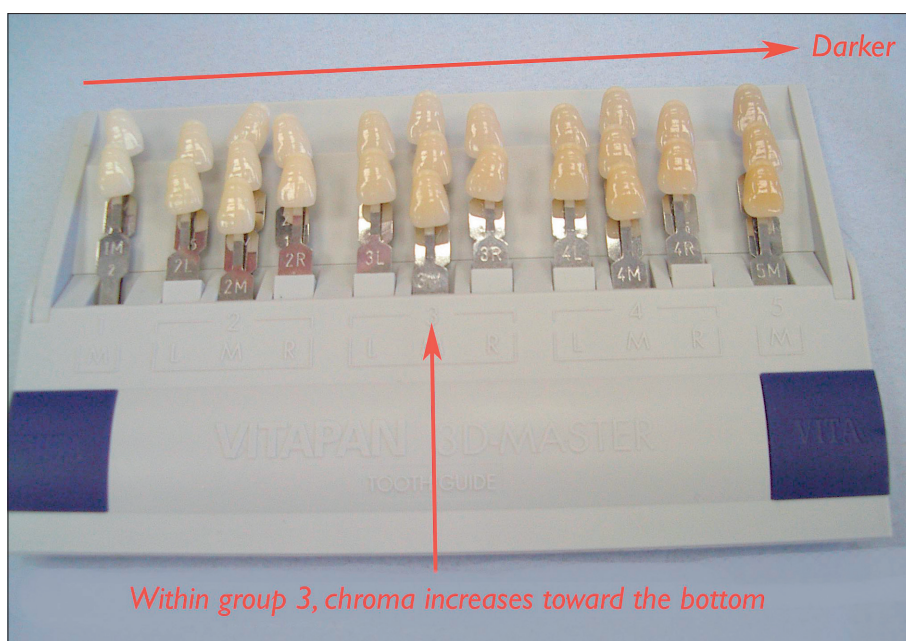
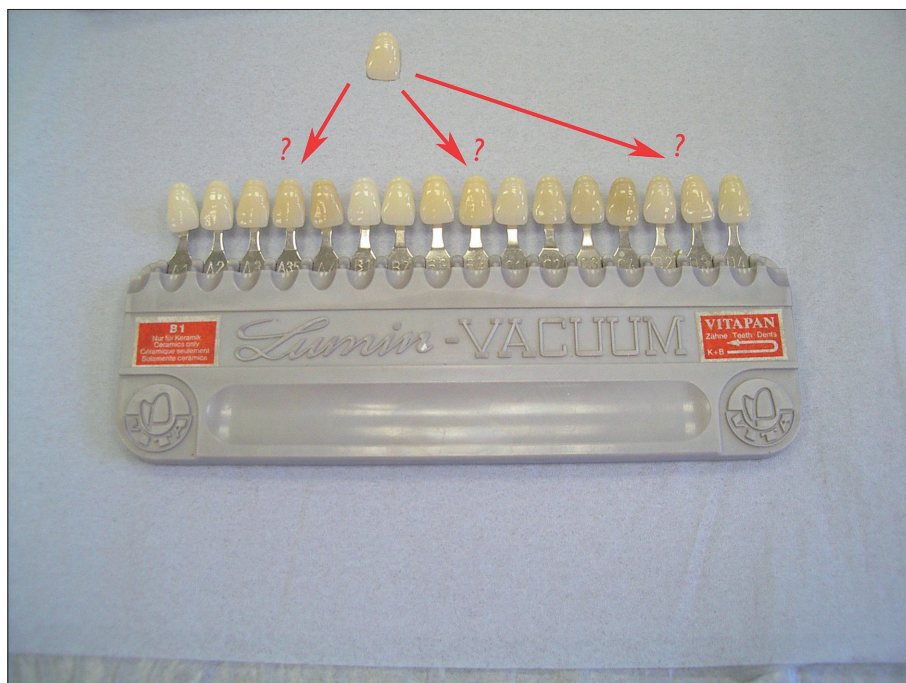
Vita's first method

Vita Zahnfabrik in Bad Sackingen, Germany, is a large dental company. They offer two arrangements.

In the first (top photo on the next page), porcelain teeth are grouped into four categories: A, B, C, and D. Notice the small letters at the base of the teeth.) Each represents a different hue. Each category is subdivided into numbers: A1, A2, A3, A3.5, A4. Here the number represents the chroma (intensity). The teeth can be arranged from lightest to darkest for comparison of value to the natural teeth.

Vita's second method

In the 3-D Master Toothguide, the shade samples are grouped in 5 lightness levels (values). (See the bottom photo on the next page.) This arrangement incorporates all three dimensions of color perception; the manufacturers claim this results in increased accuracy when selecting a shade. Value is selected first; in this example the dentist selects the three teeth labelled 3M.



The three teeth here are labelled 3M1, 3M2, and 3M3. The differences between them are higher and lower chroma (intensity). And finally, the hue is decided (L,M,R).

Color wheels

Notice how subtle this is, in comparison to ordinary color wheels. Can you see, for example, that the three teeth in the vertical row 3M differ in chroma (intensity) and *not* in value (darkness)? That the teeth in the third grouping differ in hue? The ones on the right are more red, and the ones on the left are more yellow.

This level of subtlety is beyond most instruction in art academies, where Josef Albers's *Interaction of Color* is generally considered the most detailed source. (The colors in his book are more obvious than these.)

Color sensitivity

In the original exhibition on which this book is based, we offered a model of teeth, a mirror, and a color-corrected lamp. Visitors were encouraged to compare the porcelain samples with their teeth, and see if they could name the color classifications of each of their teeth.

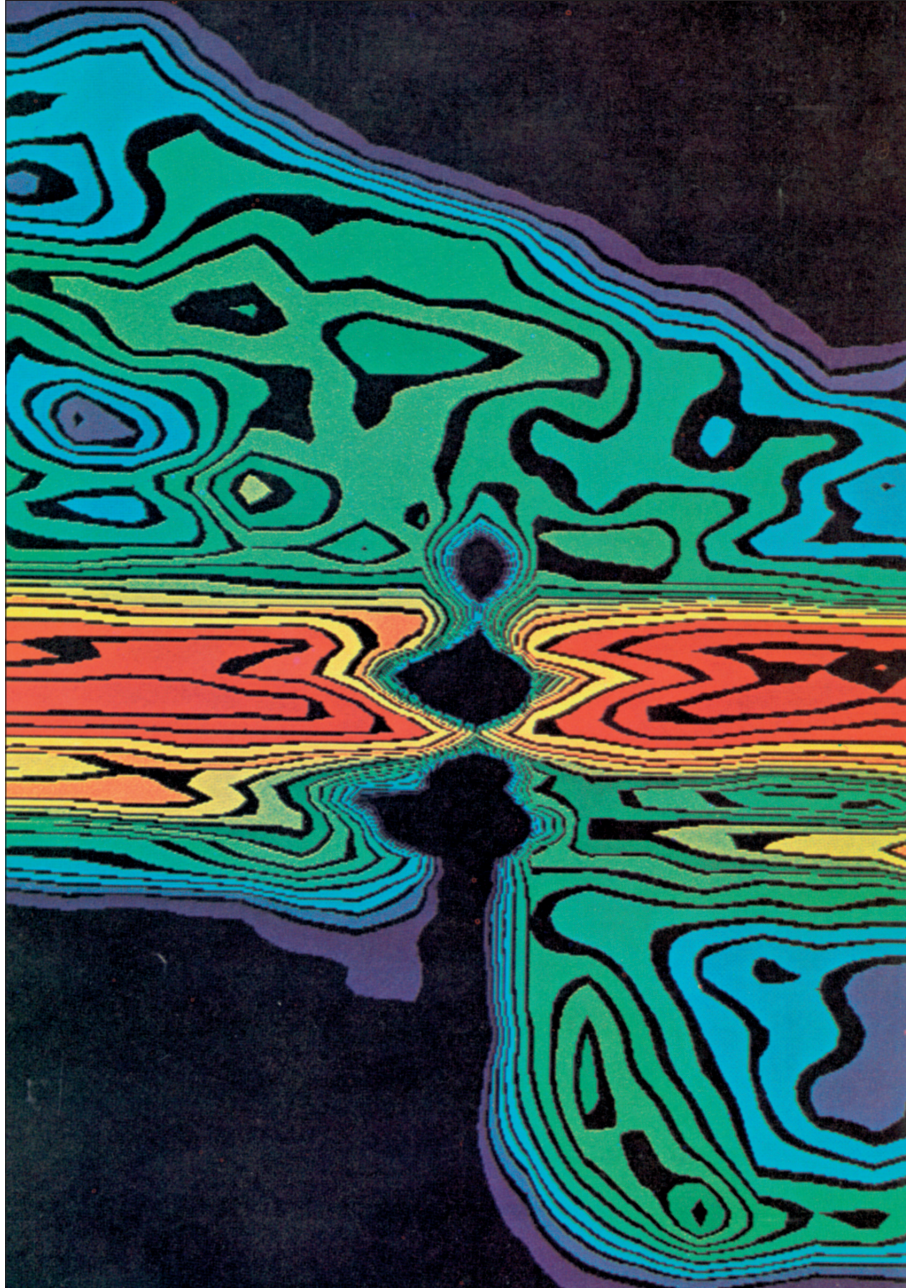


The makers of porcelain teeth recommend that dentists only compare tooth colors for five to seven seconds at a stretch, because the colors are so close in value, hue, and chroma that the eye's sensitivity begins to trail off. Very little in the art world compares with this degree of sensitivity: the closest parallel would be professional printers, who have to be very accurate in matching print runs and in approximating the colors of original prints when they are reproduced; but there is software and hardware for those tasks. In art education, Joseph Albers's *Interaction of Color* (1963) remains a standard textbook. It is used in conjunction with colored papers, and one of Albers's purposes was to increase artists' sensitivity to minute changes in hue and chroma. But even that text — in its many abridged editions and computer implementations — does not come anywhere near the precision required in matching porcelain teeth. In terms of visual subtlety and sheer discriminatory accuracy, the techniques described in this section surpass even art and history of art.

For further reading

Shimya Hobo et al., editors, *Fundamentals of Fixed Prosthodontics*, third edition (Chicago IL: Quintessence, 1997); N. Ray, "Color and Color Matching" (unpublished manuscript, 1998, University College Cork, available at www.ucc.ie/ucc/depts/restorative/downloads.htm); and R.W. Dykema, C.J. Goodacre, and R.W. Phillips Johnston's *Modern Practice in Fixed Prosthodontics*, fourth edition (Philadelphia PA: W.B. Saunders, 2001); Elkins, *How to Use Your Eyes* (New York: Routledge, 2000), chapter 27, "How to Look at Color."





12

Mapping Clouds at the Galactic Center

Gerard Wrixon, Paul Callanan, James Elkins

This image appears at first to be a naturalistic picture of something; but it is in fact a diagram. The horizontal axis is spatial — a sweep of the area just left and right of the center of the galaxy. The vertical axis, however, is coded — it records the speed at which clouds of Hydrogen are moving toward or away from the galactic center.

The image does not show visible light, but rather records the intensities of radio wave emission at the specific wavelength of 21 centimeters — so it is a non-naturalistic image that records something that is, in any case, invisible to human eyes. (This is even aside from the fact that it shows a very tiny, faint area in the constellation Sagittarius, which is almost beyond the capacity of unaided vision.)

Reading the graph

The image originally appeared in *Scientific American* in 1974, accompanied by the graphical key reproduced on the next page. To interpret the image, imagine the strip that is apparently left and right of the Galactic center: within it, gases are moving at different speeds, and at different distances from us. The red area on the image has little or no velocity: it represents the Hydrogen in our line of sight, left and right of the Galactic center. Negative values on the y axis mean gases moving toward us, and vice versa. The bit of orange and yellow at the right margin, below the red center line, named the “3-kiloparsec arm,” is a cloud of Hydrogen moving toward us at about 50 kilometers per second. The green area above, labelled “arm expanding at 135 kilometers per second,” is moving away from us.

The lower right of the image is very fast-moving Hydrogen — up to 200 kilometers per second — moving toward us, and the upper left is Hydrogen moving away. In both cases, the high velocities mean the gases are near the Galactic center.

The Center of the Galaxy

14

by R. H. Sanders and G. T. Wrixon
April 1974

Coded in the radio, infrared and X-ray emissions from the invisible nucleus of our galaxy is mounting evidence that it is periodically the scene of titanic explosions

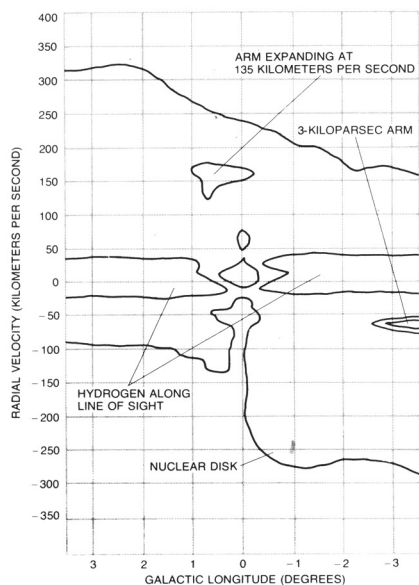
Our galaxy is a disk-shaped collection of stars, gas and dust whose components are all bound together by their mutual gravitational attraction. Like an enormous pinwheel it rotates majestically around its mysterious nucleus, or central region. From our vantage near the edge of the disk the nucleus has until quite recently been hidden by clouds of obscuring dust. Within the past 20 years, however, new techniques of "looking" through the dust have been developed, providing us with tantalizing glimpses of the nuclear re-

gion. Piecing together observations made through "windows" at wavelengths both longer and shorter than those of visible light, astronomers have become aware of striking similarities between our galactic center and the nuclei of certain bizarre objects called Seyfert galaxies.

Seyfert galaxies are named for Carl K. Seyfert, who in 1943 first classified a group of galaxies according to the unusual properties of their nucleus. They are spiral galaxies (disk-shaped galaxies with luminous spiral arms like our own

galaxy) characterized by a small, very bright nucleus embedded in rapidly moving masses of gas that are apparently being ejected from the central region. Seyfert nuclei are also a rich source of infrared radiation and radio waves. Indeed, Seyfert nuclei emit such large amounts of energy and matter that our present laws of physics may be inadequate to explain them.

Quasars, which were discovered in the early 1960's, may be even more extreme examples of the phenomenon seen in Seyfert galaxies. Quasars are very



GAS MOTIONS AT GALACTIC CENTER are displayed in the computer-generated contour map on the opposite page. Based on observations made with the 140-foot radio telescope of the National Radio Astronomy Observatory at Green Bank, W.Va., the map shows the distribution of emission from un-ionized hydrogen at a wavelength of 21 centimeters. The different colors indicate the intensity of the 21-centimeter line, ranging from violet (lowest level) to red (highest level). The vertical axis, as shown at the left, does not indicate galactic latitude but rather the velocity of hydrogen lying in the galactic plane: velocities toward us are negative, velocities away from us are positive. The horizontal red ridge centered at zero velocity represents all the un-ionized hydrogen along the line of sight on either side of the galactic center. The deep hole at the center identifies where 21-centimeter radiation from the powerful radio source known as Sagittarius A is absorbed by un-ionized hydrogen lying between it and us. To the right and just below the central ridge, at a negative velocity of more than 50 kilometers per second, is a fainter ridge produced by emission from the "three-kiloparsec arm." Since the three-kiloparsec arm also produces an absorption line in the output of Sagittarius A, the arm is on this side of the center, and since its velocity is negative it is expanding away from the center and toward us. At the lower right there is a ridge of emission (blue-and-green feature) whose maximum velocity exceeds 200 kilometers per second. This ridge is emission from the nuclear disk; its high velocity means that it is very near the galactic center and rotating rapidly. Notice that the velocity approaches zero toward the galactic center. Above and to the left of the center the picture is somewhat ambiguous. The dominant feature is a ridge of emission (green band) that crosses the position of the galactic center at +135 kilometers per second; hence it is an expanding arm of gas moving away from us. The absence of an absorption hole at the position of Sagittarius A means that the expanding arm is on the other side of the nucleus. The program for generating the color contour map was devised by Thomas Cram and David Ehnebuske.

In three dimensions

Because we are more or less in the Galactic plane, we see the center edge-on. The image therefore encodes a picture of gases rotating around the center, like the spiral arms of stars in the Galaxy as a whole.

Very high-velocity Hydrogen is rotating close in to the center. Lower-velocity Hydrogen is farther away: one arm swings around toward us, on the right; and a second swings away from us on the left. It is not easy to visualize this, but it is a typical exercise in scientific illustration.

The limits of the image

There are, perhaps, two limitations to this image. First, it has relatively few data points. The isobars are really line segments (made jagged by the large pixels) that connect one data point to the next. That is an insuperable limitation because 21-centimeter radio emissions cannot be made more detailed.

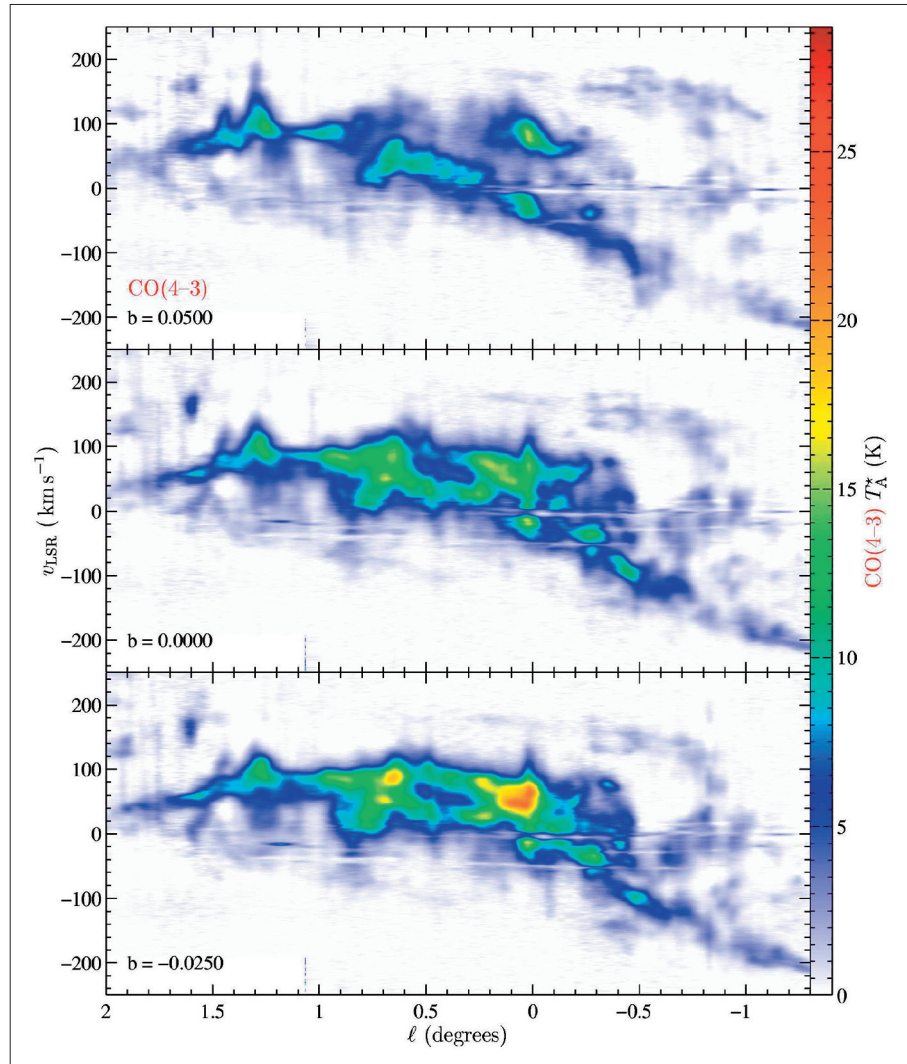
Another limitation comes from the *use* the image was meant to have. In 1974 the idea of black holes was new. To test whether or not a black hole might be present, Sanders and Wrixon made a “model galaxy” simulation on a “large electronic computer” and “observed” it as they observed the actual Galaxy. By changing the mass of the central object, and seeing how the model matched their image, they concluded that whatever lies at the Galactic center could be as large as 200 million solar masses — within the range of a black hole. Thus the image was augmented by a computer model, and would have been incomplete without it.

2004

The first of these limitations — resolution — is easily improved by searching for emissions other than 21 centimeter Hydrogen emissions. Carbon monoxide, for example, has several characteristic emission wavelengths, among them 0.065 centimeters (461 GHz), which are caused by a particular quantum jump in the atoms, from $J = 4 \rightarrow 3$.

In 2004, thirty years after Sanders’s and Wrixon’s study, a team led by Christopher Martin produced the images reproduced below. Each frame is a longitude-velocity graph like Sanders’s and Wrixon’s; the middle one samples the Galactic center, and the others show the level (galactic latitude) just above and below it.

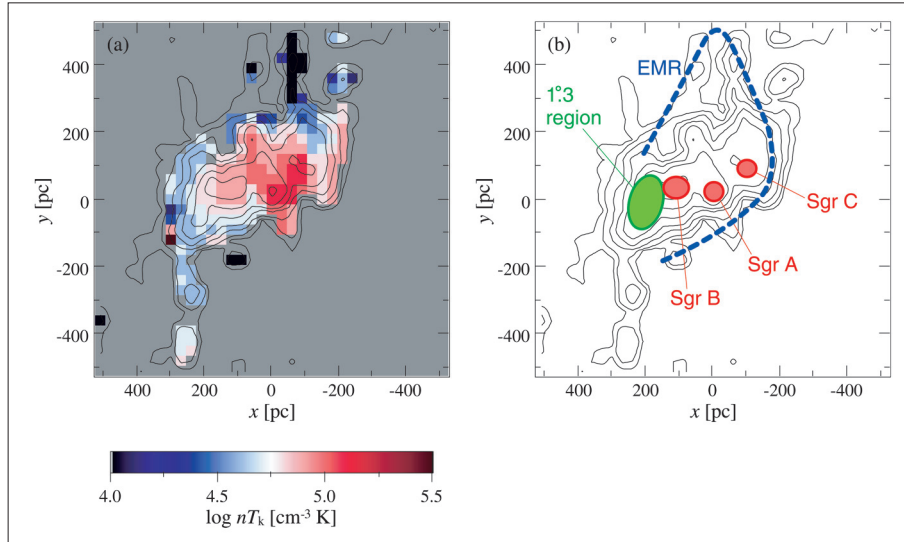
The left-right range in degrees is about the same as Sanders’s and Wrixon’s diagram, but the smaller wavelength allows much higher resolution. Because these images sample carbon dioxide clouds and not hydrogen, they are hard to compare with the 1974 diagram — and they hint at the complexity of the region.



Face-on views

Another recent development is the computer-aided calculation of face-on views, showing the Galactic center “from above.” One is shown here.

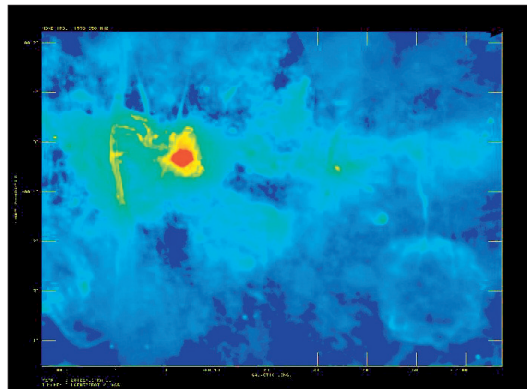
The center is now known to be comprised of at least three sources, known as Sgr A*, B, and C, and they orbit the Galactic center. This image records gas thermal pressure in another emission line of carbon monoxide. The authors of the study posit a model with four bodies (Sgr A*, B, C, and an object known as the “1.3° region”) rotating around one another in two or more spiral arms.

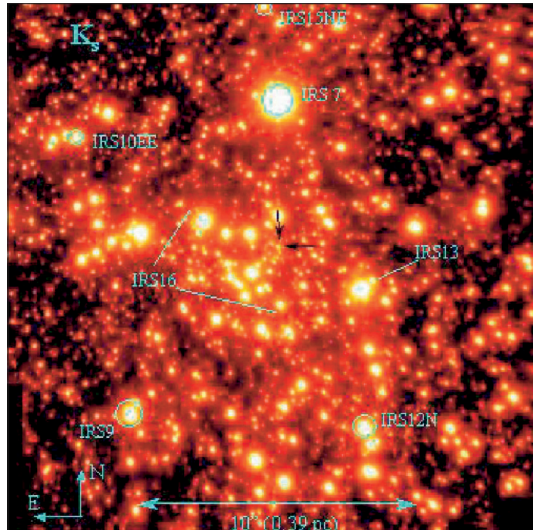


Clouds, shells, arcs...

Martin notes that the region close to the Galactic center has “a complex distribution of emission, which is chaotic, asymmetric, and non-planar, [with] hundreds of clouds, shells, arcs, rings, and filaments.” (A little farther from the center, at the distances studied by Sanders and Wrixon, the new study confirms “the gas is loosely organized around closed orbits.”) There are even star clusters near the center, named “the Arches” and “the Quintuplet.” The picture is gradually becoming more complex, if not clearer.

This photo is another radio-frequency image, at 1.4 GHz. F. Yusef-Zadeh, who published this image on January 15, 2005, compares the Galactic center to “a jungle where many species evolve, share the same resources and interact with each other.”



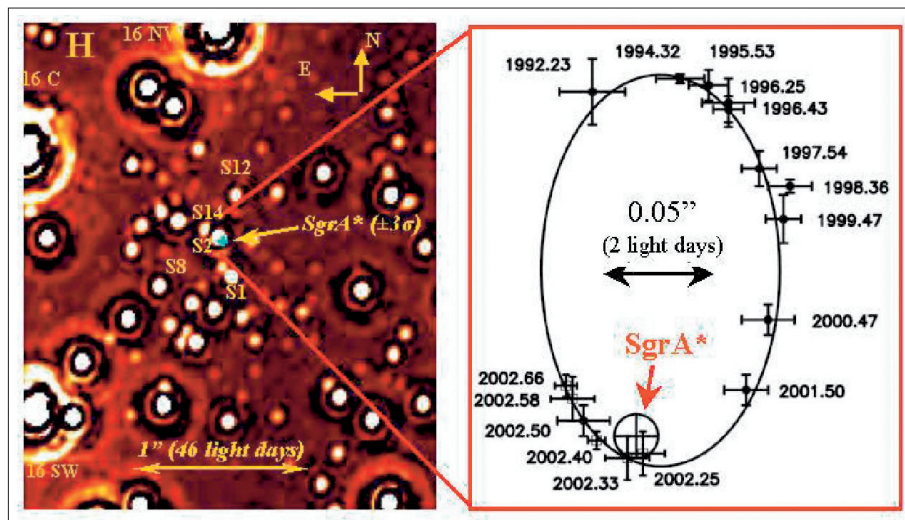
Optimal resolution

Recently, too, there has been interest in “non-thermal filaments” (NTFs), long, thin clouds that are only found near the Galactic center. Astronomers have managed to map them in detail even though they are less than an arcminute in apparent length — that is less than one-sixtieth the width of one of the grid squares in the *Scientific American* graph. (For comparison: one arcminute is one-thirtieth the diameter of the full Moon — a tiny portion of the sky.)

Yet there is no way to achieve

perfect resolution of nebulous objects, because the objects themselves have arbitrarily defined boundaries.

Point-like objects are another matter, and studies of stars at the Galactic center are well advanced. Infrared studies of stars have achieved amazing resolutions. Photo above is about 20 arcminutes wide, about the size of the central black area in the first image.



The bottom photo on the last page, in turn, is a detail of that tiny portion, zooming in on the enigmatic Sagittarius A (marked Sgr A^{*}). The arrow shows the scale: one arcsecond, which is one-sixtieth of the width of one of the squares in the 1974 image. At that resolution it is possible to plot individual stars as they orbit around Sgr A^{*}. (As this book goes to press, scientists at the Max-Planck-Institut für extraterrestrische Physik have released a movie of the motion of the stars in this region, pushing the limits of resolution still further).

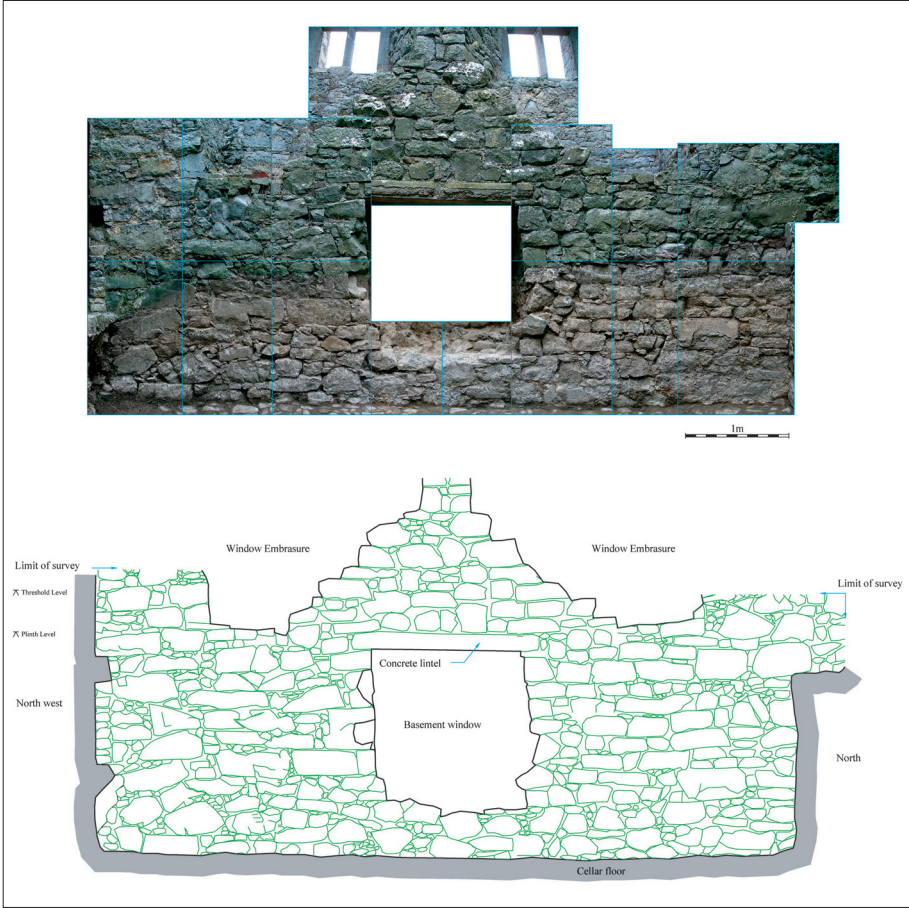
What comprises a perfect image?

The conundrum here is the resolution of irresolvable objects. The same problem is of concern in images of the earliest pre-galactic objects at the edge of the visible universe, which will be targets of the Next Generation Space Telescope: they overlap and have no distinct boundaries. What is required is a mathematical constraint on what counts as an “object”: a situation far from the concerns of image making in daily life or in art.

Of these images, the one that is most strongly counter-intuitive is the first, because it only appears to be a picture like some later ones. It is, rather, a graph posing as a naturalistic picture — asking to be read, illegitimately, as a picture — a theme that recurs in several of these chapters.

For further reading

Chrisopher Martin et al., “The AST/RO Survey of the Galactic Center Region. I. The Inner 3 Degrees,” *ApJS* 150 (2004): 239, plate 6; Tsuyoshi Sawada et al., “A Molecular Face-on View of the Galactic Centre Region,” arXiv:astro-ph/0401286 v1 15 Jan 2004, Fig. 11; F. Yusef-Zadeh et al., “Starburst Driven Thermal and Non-thermal Structures in the Galactic Center Region,” Fig. 1; T. Ott et al., “Inward Bound: Studying The Galactic Center With Naos/Conica,” figs. 1 and 4. See also T. Viehmann et al., “*L*- and *M*-band Imaging Observations of the Galactic Center Region,” arXiv:astro-ph/0411798 v1 30 Nov 2004, and Johannes Staguhn et al., “350 μ m Galactic Center Dust Observations with SHARC II,” arXiv:astro-ph/0412148 v1 6 Dec 2004. For the movie of the stars and the galactic center, see www.mpe.mpg.de/ir/GC/prop.html.



13

The Repertoire of Archaeological Images

Hugh Kavanagh

Archaeology, it could be argued, is one of the most visually-oriented and visually intensive disciplines in the university. Much archaeological research is carried out by inspecting maps and plans of previously recorded monuments. Newly discovered sites are meticulously mapped and recorded using a variety of media and methods.

The visual methods of archaeology range from wholly automated images (for example, aerial photographs) to freehand drawings. Here is a sample.

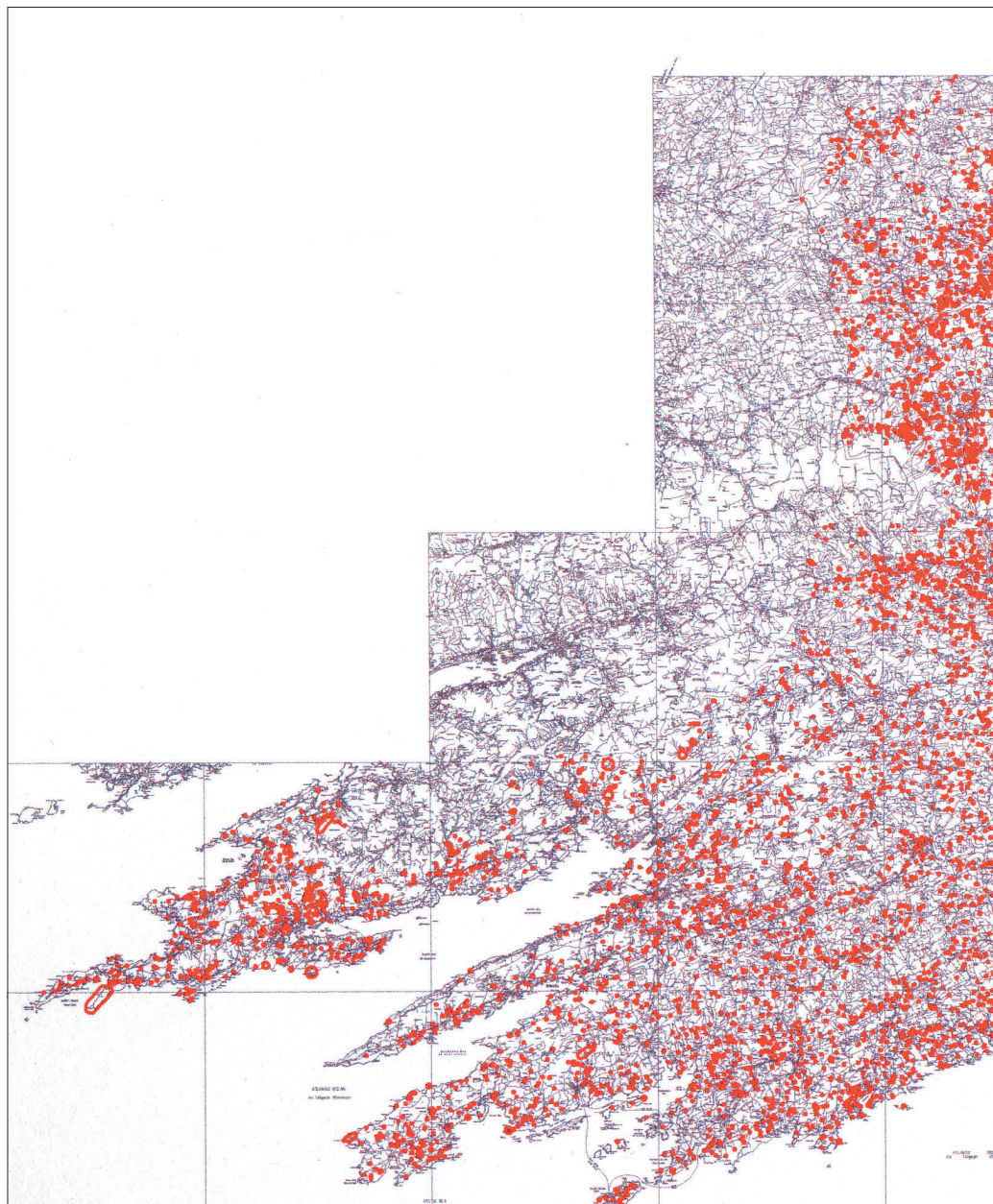
Cumulative mapping

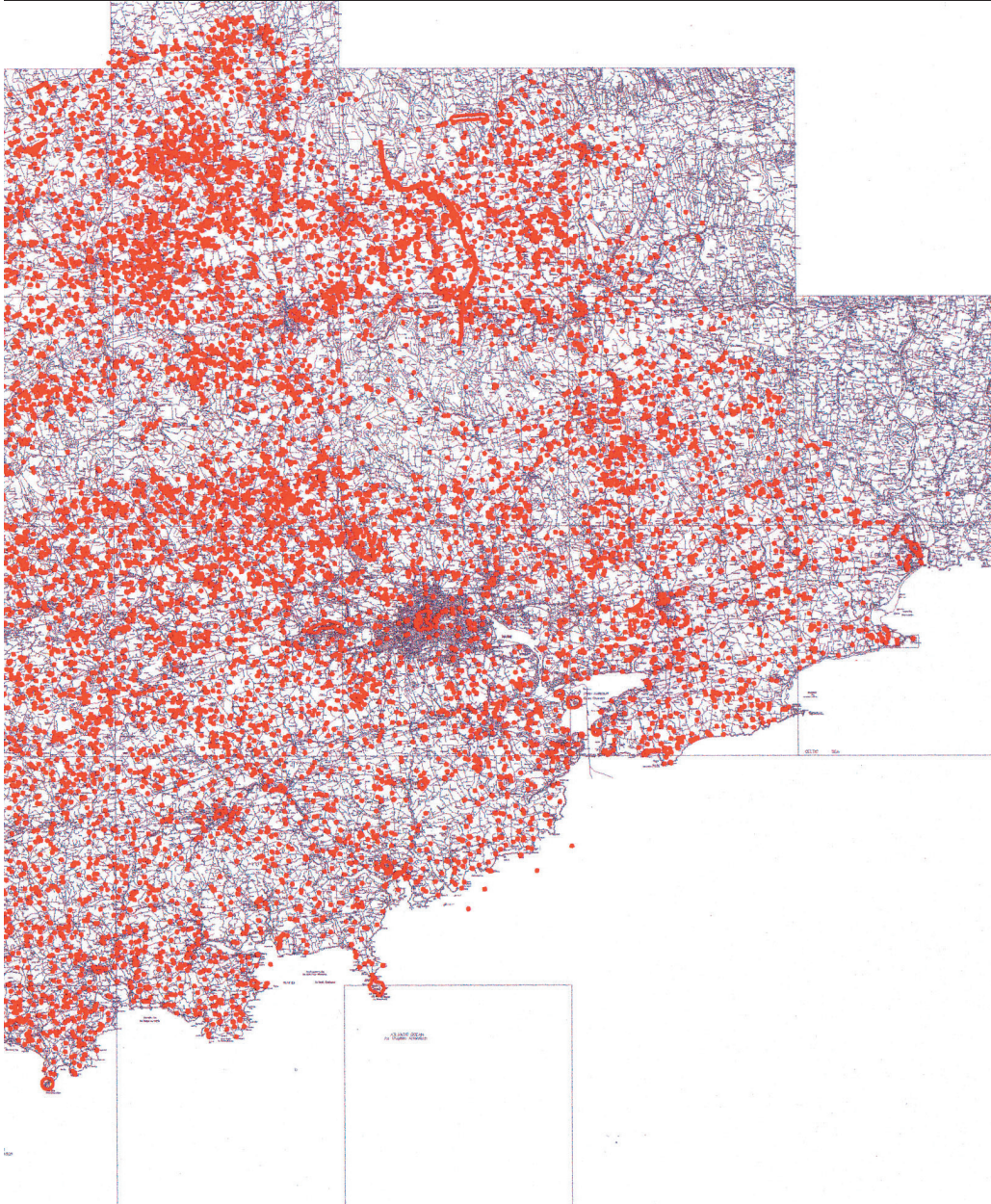
Archaeologists record the exact position of sites using Global Positioning data. Large compendia of archaeological sites will often give these data, called GIS, for Geographic Information Systems. (Global Positioning data has been abused in the United States by people who use them to find and loot remote sites.)

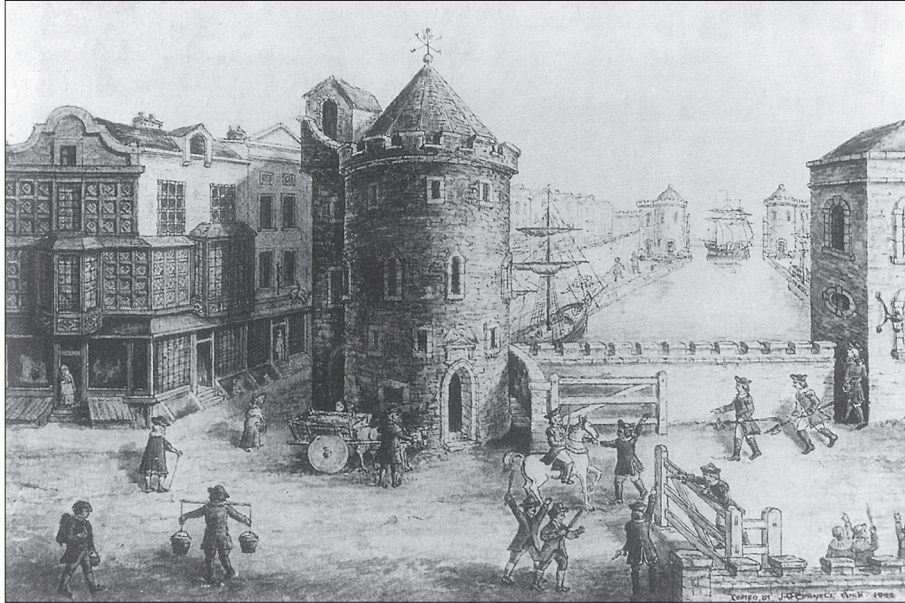
The image on the next two pages was made by overlaying GIS information from the Heritage Service onto an Ordnance Survey vector map, at a scale of 1:50,000. It shows every archaeological site in County Cork, Ireland. That kind of manipulation can be done using automated software — in this case, AutoCAD Map 2004.

Older images

At the other end of the time scale, archaeologists make use of historical images. The image on nineteenth-century copy of an earlier painting looking down along what today is Castle Street, Cork. The painting shows a ship entering the city between the King's and Queens castle: a motif that was repeated in the Cork city coast of arms.







Development planning

Archaeologists are commonly involved in issues of planning.

This AutoCAD drawing on the next page combines four sources:

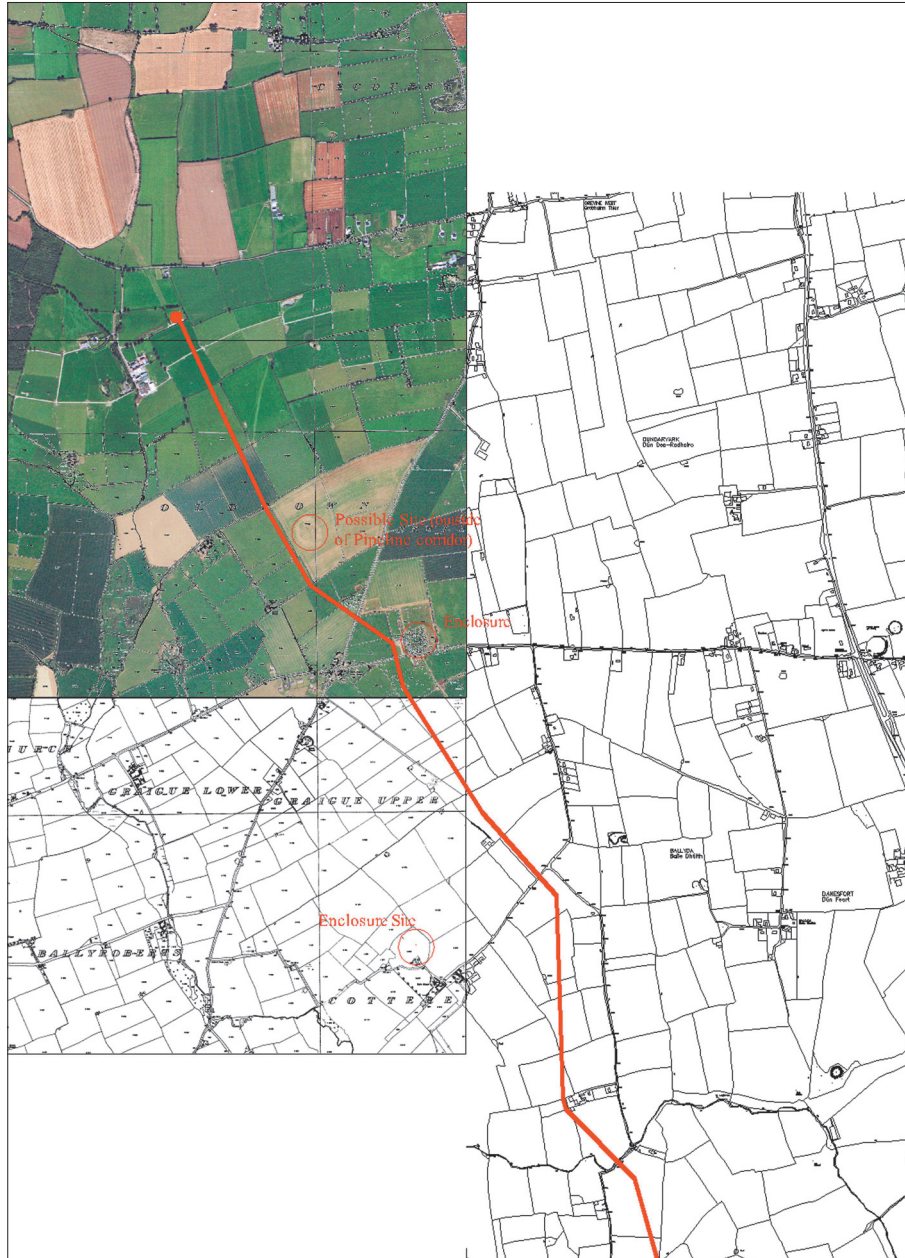
1. Geo-referenced aerial mapping (upper left)
2. Second- and third-edition Ordnance Survey mapping (lower left, right)
3. Technical development drawings from the client (red line)
4. GIS information from the Department of the Environment, Heritage and local government (circled).

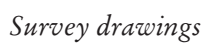
Combining this graphical information aids the archaeologist in advising developers where archaeological impacts can be avoided or minimized. In this case, the subject is a proposed gas pipeline.

Urban sites

The image on page 146 depicts excavations are being carried on at 35-39 Main Street, Cork, behind the city library.

This drawing shows the excavation in relation to an Ordnance Survey map at a scale of 1:1,000. Note the detail: every street address is given. *Mh* stands for “manhole”; *LS* for “light standard.”

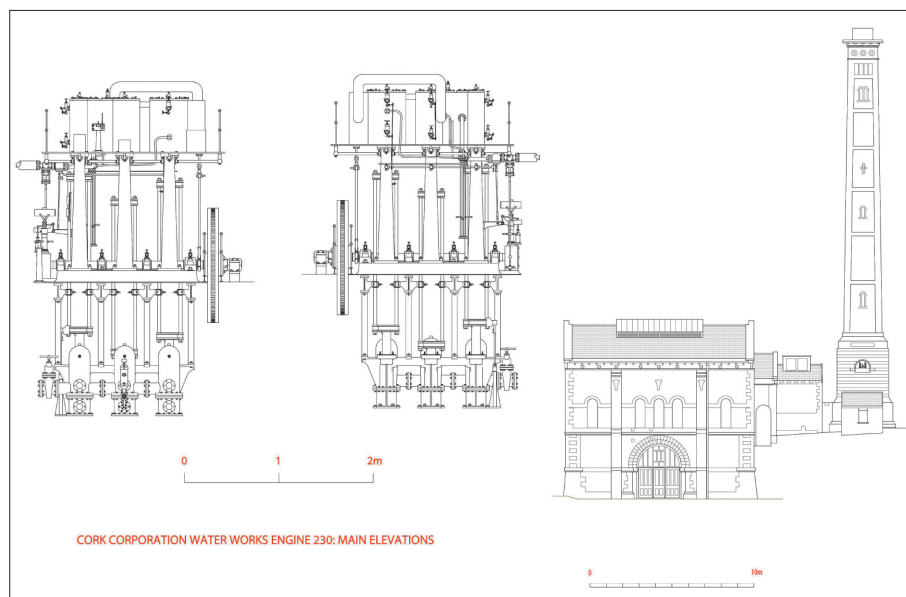




At times archaeologists use skills associated with architects and engineers, as in this study of the Cork Waterworks. The Adobe Illustrator drawing on page 147

shows two examples of building survey techniques. The chimney elevation is carried out using traditional surveying methods and also using a surveyor's "EDM total station" (*EDM*, for "electromagnetic distance measuring": lasers calculate distances automatically).

The steam engine elevation was created by extrapolating details from a 3D "point cloud" measured by a laser scanner. (For more on laser scanners, see Chapter 22.)



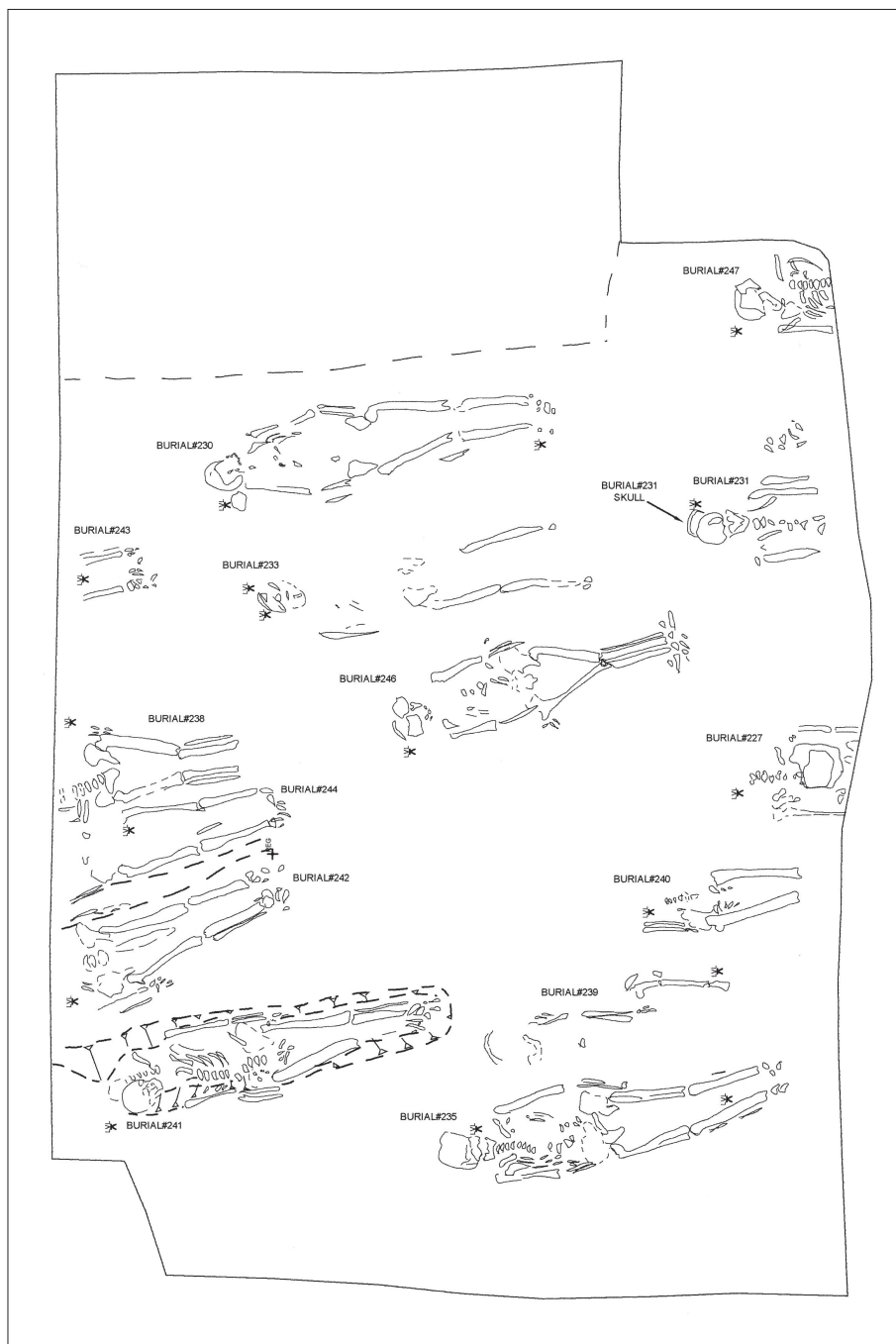
Photogrammetric surveys

Another way to create an elevation is by "rubbersheeting" many separate digital photographs to make an accurate, undistorted photographic elevation.

The image reproduced at the beginning of this Chapter shows a wall at Burncourt Castle, Co. Tipperary. Fixed points were surveyed using a "total station"; those points then corrected the mosaic of digital photos. Notice that the wall with windows is distorted: it is beyond the picture plane of the corrected wall.

Technical plans

The image on the next page is a technical *in situ* plan, originally drawn in pencil on drafting film (a kind of paper made from duralar polyester that is used in technical drawing), using grid lines and coordinates. The pencil

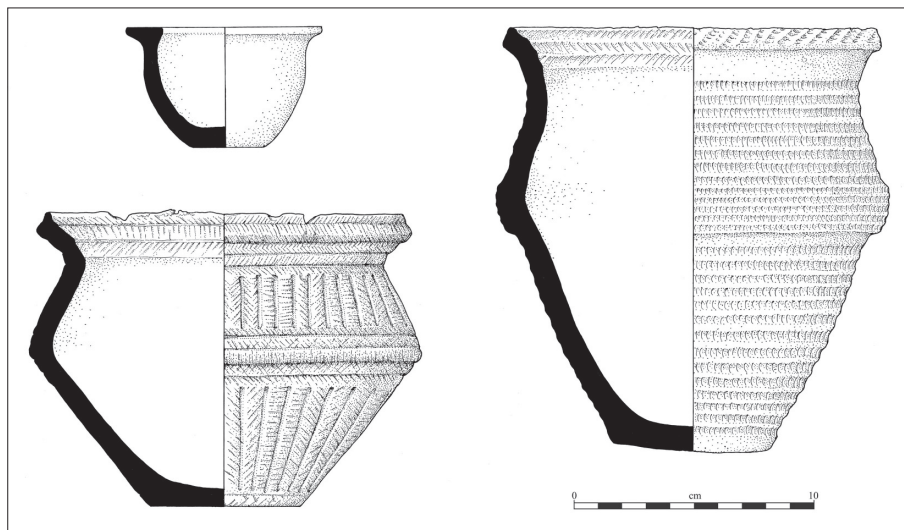


drawings were then converted into digital formats, as shown. (In the past, the pencil would have been gone over with permanent ink.)

Measured drawings

Another kind of drawing that is hand-done is the cross-section and elevation of individual objects, like these Bronze Age pots found at Castlehyde, Fermoy.

The details displayed here may only be obvious to a trained archaeologist, any superfluous details that might seem important to a casual observer are omitted. In other words, they are not simply realistic but selective in what they record.



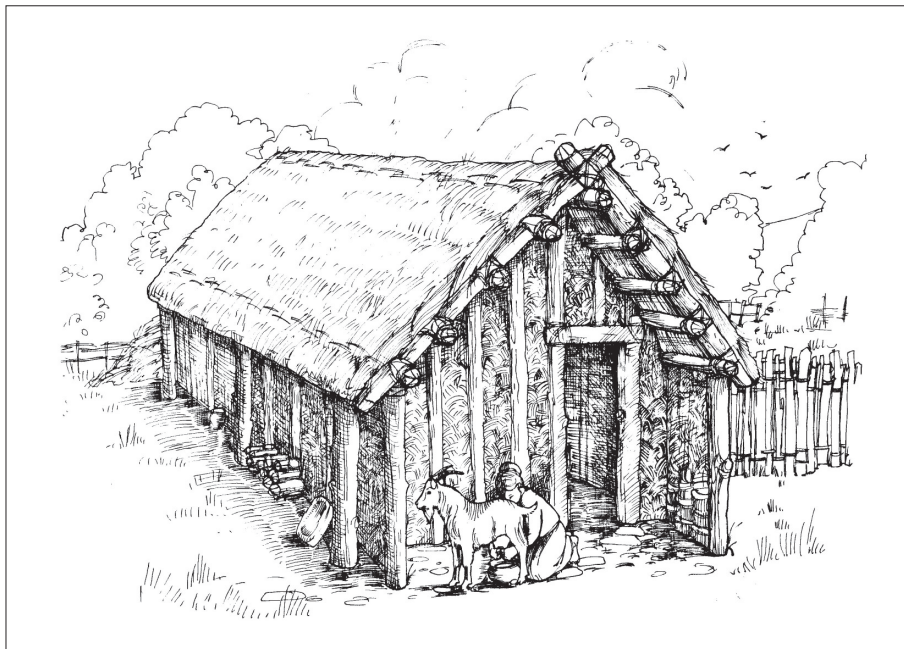
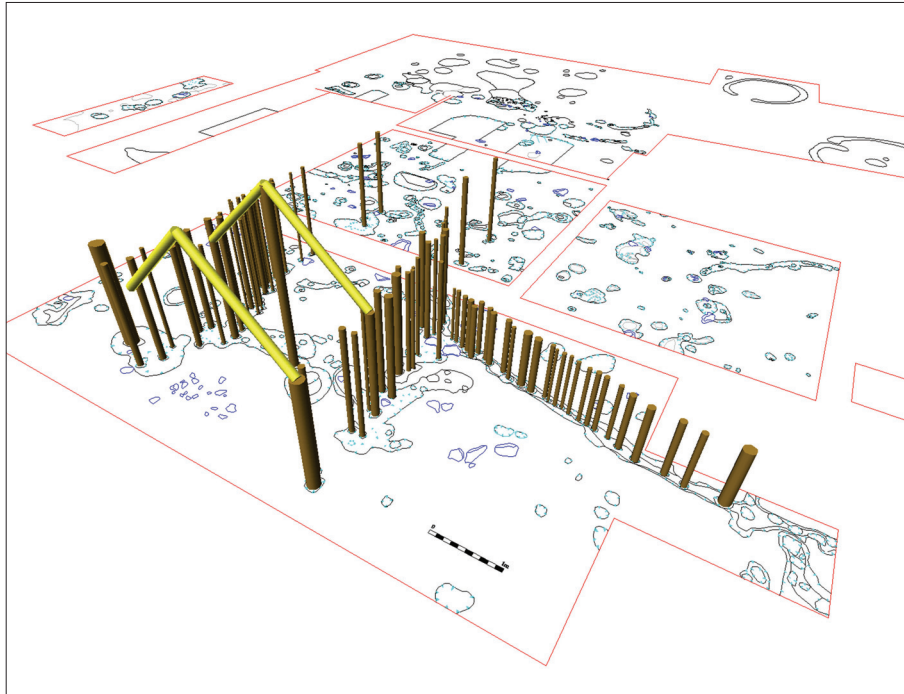
Computers versus hand drawing

Freehand drawing has a marginal, but essential place in several disciplines. In archaeology it can complement computer-assisted mapping.

The two pictures on the next page show a Bronze Age house at Curraghatoor, Co. Tipperary. The computer-assisted design has a speculative elevation (all that is known for sure is the positions of the bases of the stakes and posts). A freehand reconstruction restores a sense of scale and eliminates the intrusive detail typical of CAD (computer-assisted design).

Compatibility and the “thicket of images”

Some kinds of imaging work perfectly together; others are stand-alone. In that respect archaeology resembles the study of viruses, where no one kind of image



will do (that theme is also exemplified in Chapter 27, and elaborated in the Introduction). There are interesting parallels between disciplines that require multiple kinds of pictures: they each involve objects that have more than one level of detail (like fractal objects, they change depending on how closely they are observed); and they involve technologies that only work at certain scales (move in too close to a virus, and you need a different kind of microscopic technique; move in too close to an archaeological site, and you need a new map). It would be interesting to develop a general theory of such incompatibilities: a possible project for a future image science.

Emotional power



But all these techniques come down to the subject matter of archaeology: people's lives. The excavation of skeletons in particular is an emotional subject, but it must be carried out in the most accurate and objective manner possible. That is one of the paradoxes of archaeology: its battery of scientific illustrations can be used to capture the most personal and moving subjects.

Some of the finds result in images of extraordinary power, strangely at odds with the desiccated, scientific images that preceded them. In this case the subject is a burial site in which a woman's child is interred between her legs.

For further reading:

Ken Dark, *Theoretical Archaeology* (Ithaca NY: Cornell University Press, 1995); *The Student's Guide to Archaeological Illustrating*, edited by Brian Dillon (Los Angeles: University of California Press, 1985); Lesley and Roy Adkins, *Archaeological Illustration* (Cambridge NY: Cambridge University Press, 1989); and www.gisuser.com.au/MM/content/2001/MM16/feature/MM16_feature.html.



14

A Geological Map

Ivor A. J. MacCarthy

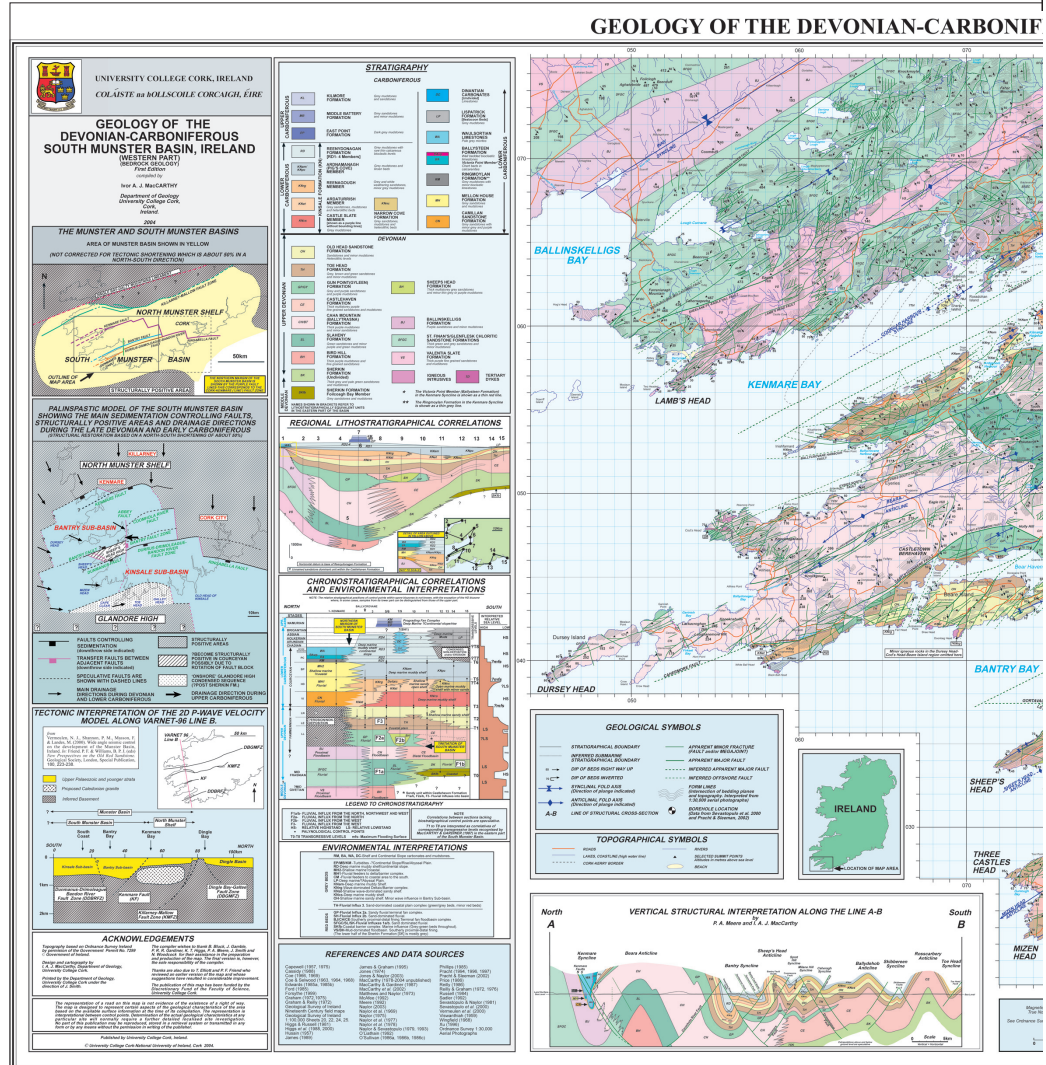
Geologists' maps are concentrated repositories of information, like non-visual databases in some other disciplines. Nominally, they present the distribution of various geological formations on the Earth's surface; they are based on examination of rock outcrops, but also on subsurface information such as boreholes and geophysical surveys.

In addition, they have a theoretical aspect; it lies partly in the fact that the geological composition of areas lying between data points must be interpreted. Maps also contain theoretical models of the structural composition and past environments in a region, and they model factors which may have affected sedimentation patterns during the infilling of ancient sedimentary basins.

Geological map of the South Munster Basin

This map describes and interprets the geology of the western part of the South Munster Basin in Ireland. This area was part of a large sedimentary basin measuring about 150km by 90km, which developed as an area of subsidence towards the end of the Devonian Period about 360 million years ago, much like the Lake Eyre Basin of Australia or the Tarim Basin of Tibet. Subsidence continued here until the middle of the Carboniferous Period, about 315 million years ago. The basin accumulated about 5km of sediment during that time in response to the varying environmental conditions, which were strongly influenced by climatic factors and fluctuations in global sea level. Subsequently, at the end of the Carboniferous Period (about 290 million years ago), the sediments infilling the basin were deformed by titanic plate tectonic forces which resulted in their deformation. This took the form of intense folding and fracturing. The deformed fill of that sedimentary basin now constitutes the bedrock of southern Munster.

The main map shows the distribution of the various rock types comprising the bedrock. The colours represent distinctive rock types or formations. Each formation is given a code which assists its identification in the Stratigraphy legend.

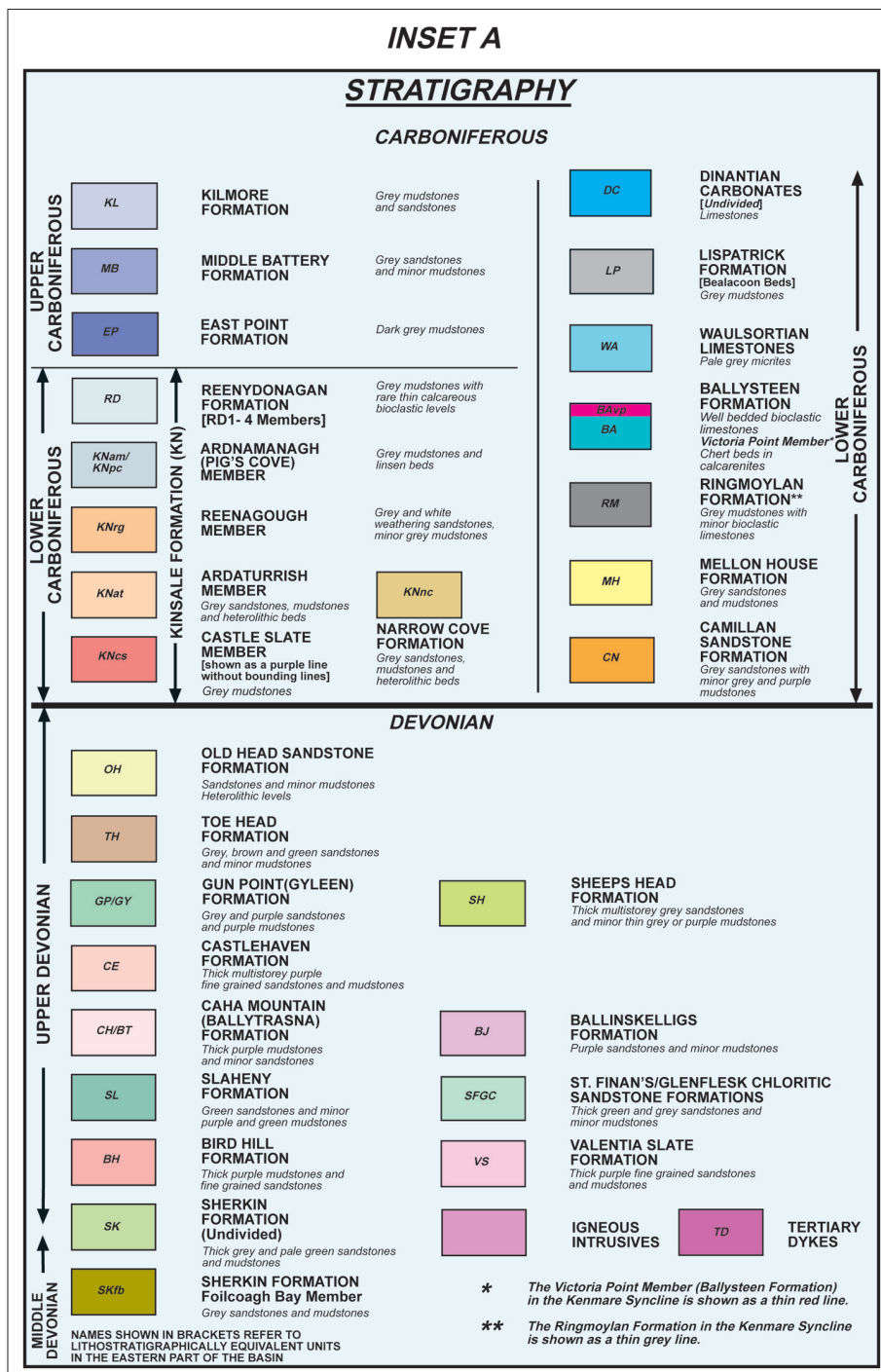


The map also shows a number of structural features such as faults and fractures in the bedrock. Also shown are the axes of folds such as anticlines (N-shaped folds) and synclines (*-shaped folds). The dip or inclination of the sedimentary layers is also shown. The thin black lines show the intersection of the layers with the surface, and are known as form lines.

[illegible]

The boxes on the left-hand side and along the lower margin of the map provide further information on the geology of the area.

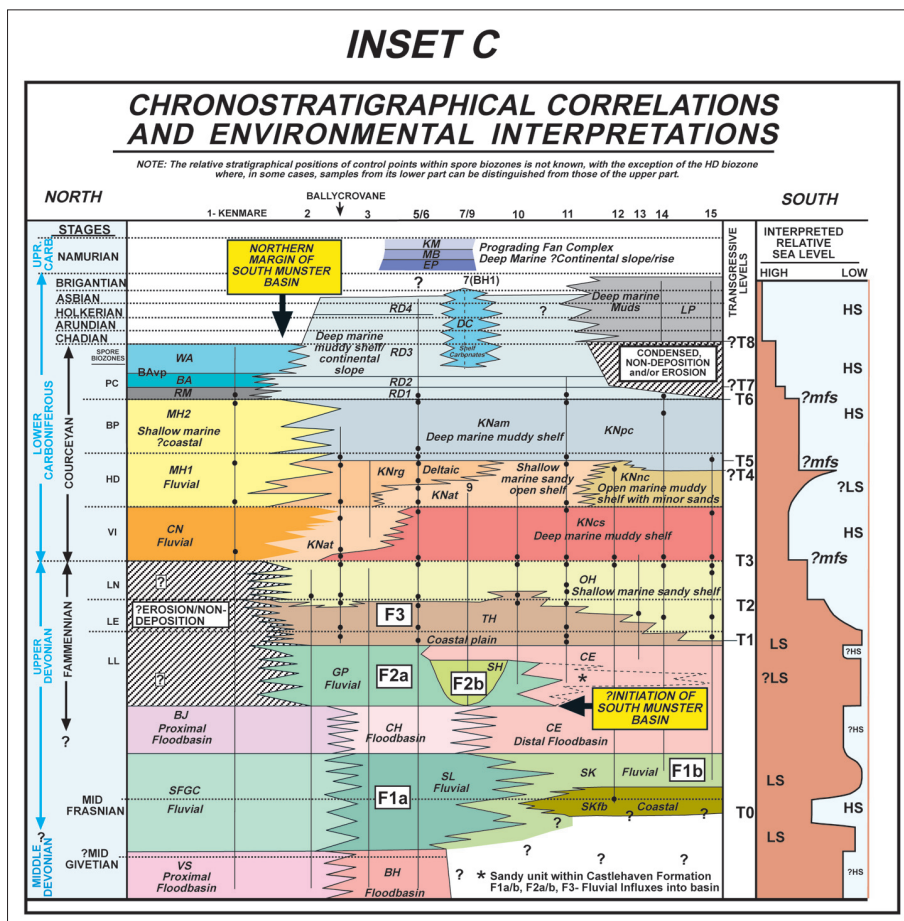
The various coloured parts on the map show the areas underlain by particular rock types or formations. The legend shown on the next page identifies and describes these



formations and lists the order in which they were laid down. The oldest layers are at the base of the legend. The rock layers become younger as one ascends this legend. Each formation is given a two-letter code, which also appears on the map for ease of identification. The legend also gives a brief description of each formation in terms of its rock type. Also shown here are the geological ages of the rock formations.

Regional lithostratigraphical correlations

Just under the stratigraphy key is a drawing that shows what the rock layers would have looked like if a vertical section had been made across the basin after the rocks were deposited but before they were deformed at the end of the Carboniferous Period. The drawing shows how the thickness of the layers changes across the basin in a rough north-south direction. A scale bar is shown on the



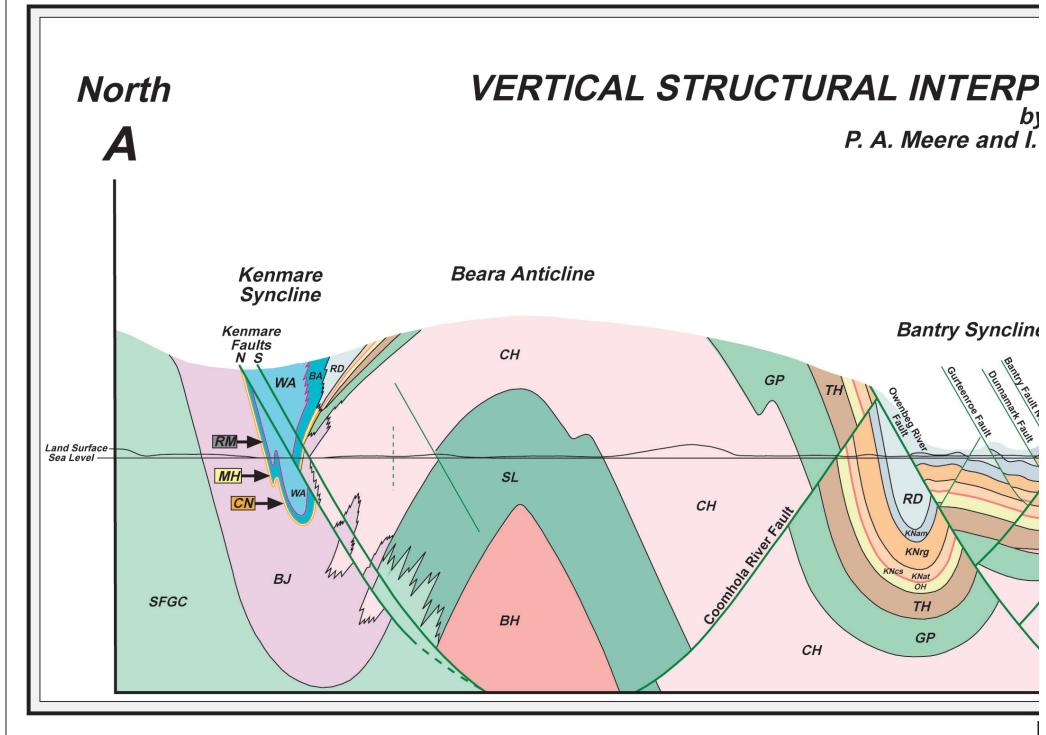
INSET D

diagram for the vertical thickness (the scale is exaggerated for clarity). The smaller inset map shows the line of section and the data points.

Chronostratigraphical correlations and environmental interpretations

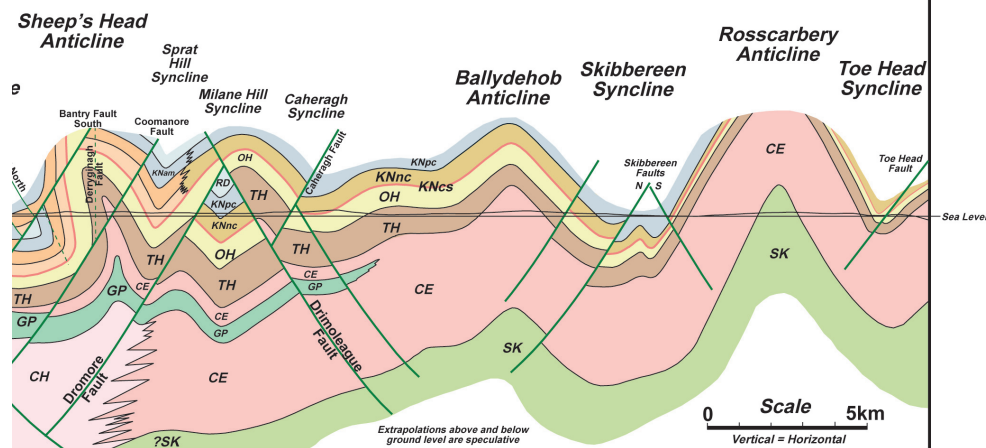
The legend reproduced on the previous page lists the full range of rock layers or formations according to their age, the formations becoming younger as one ascends the diagram. It also shows how the various formations change laterally across the basin. The vertical axis on this diagram represents geological time rather than thickness. The horizontal axis is distance. The various geological time intervals, known as “Stages”, are listed on the left hand side of the diagram. These are determined by examination of fossils, in particular microfossils. These are shown as “Palynological control points.” Palynology is the study of fossil plant spores and can be used to determine the relative age of sediments and their environment of deposition.

The diagram also presents interpretations of the environmental conditions which are thought to have been responsible for the deposition of the various rock forma-

RETATION ALONG THE LINE A-B

A. J. MacCarthy

South
B



tions. Importantly, the diagram presents an interpretation of the relative sea level (rising or falling) during the course of the basin's history. This is the brown-colored graph on the right of the diagram. HS indicates relative high stands of sea level and LS represents relative low stand of sea level. T1 to T8 represent a number of "marine transgressions" or inundations into the area. "Maximum flooding surfaces" mark the farthest landward advance of the sea during a marine transgression. The diagram also shows the times when there were major influxes of sediment (F1, F2, F3) into the basin from the land located to the north and west at this time.

Vertical structural interpretation along the line A-B

This drawing allows one to understand the folding of the rock layers. It represents a side view of an imaginary vertical slice through the landscape. The slice goes from point A to B on the main map. The land surface is shown as a wavy line. It runs just above and below the straight horizontal line indicating sea level. The colors on the cross section correspond to the colours on the main map. If the wavy horizontal

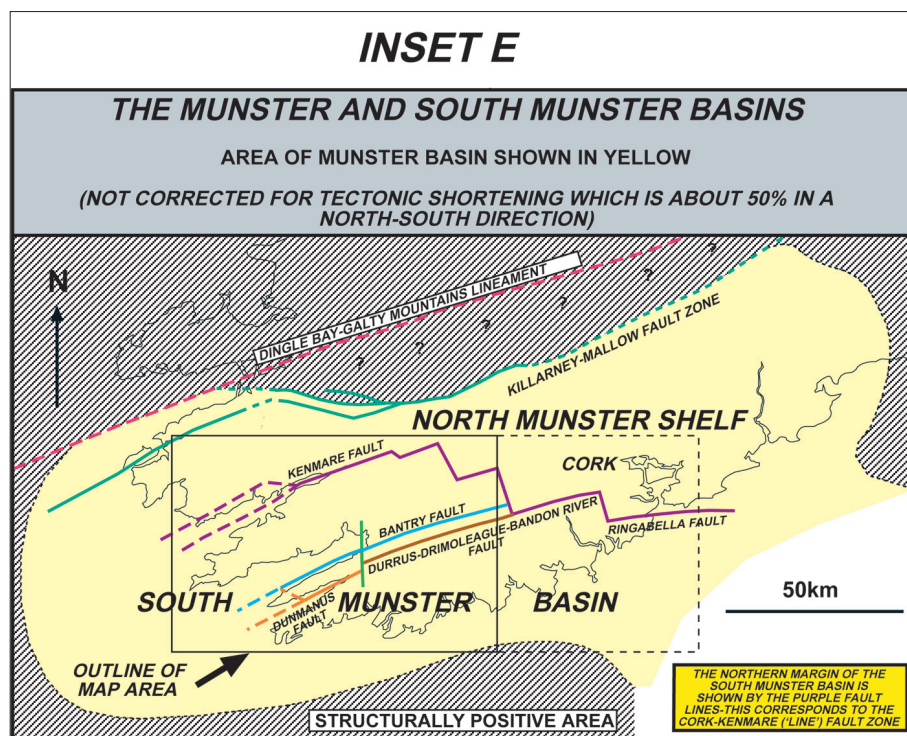
line is followed the same succession of colors are encountered as one follows the line from A to B on the main map. This diagram also extrapolates upwards and downwards where the rock formations are thought to have been located.

The Munster and South Munster Basins

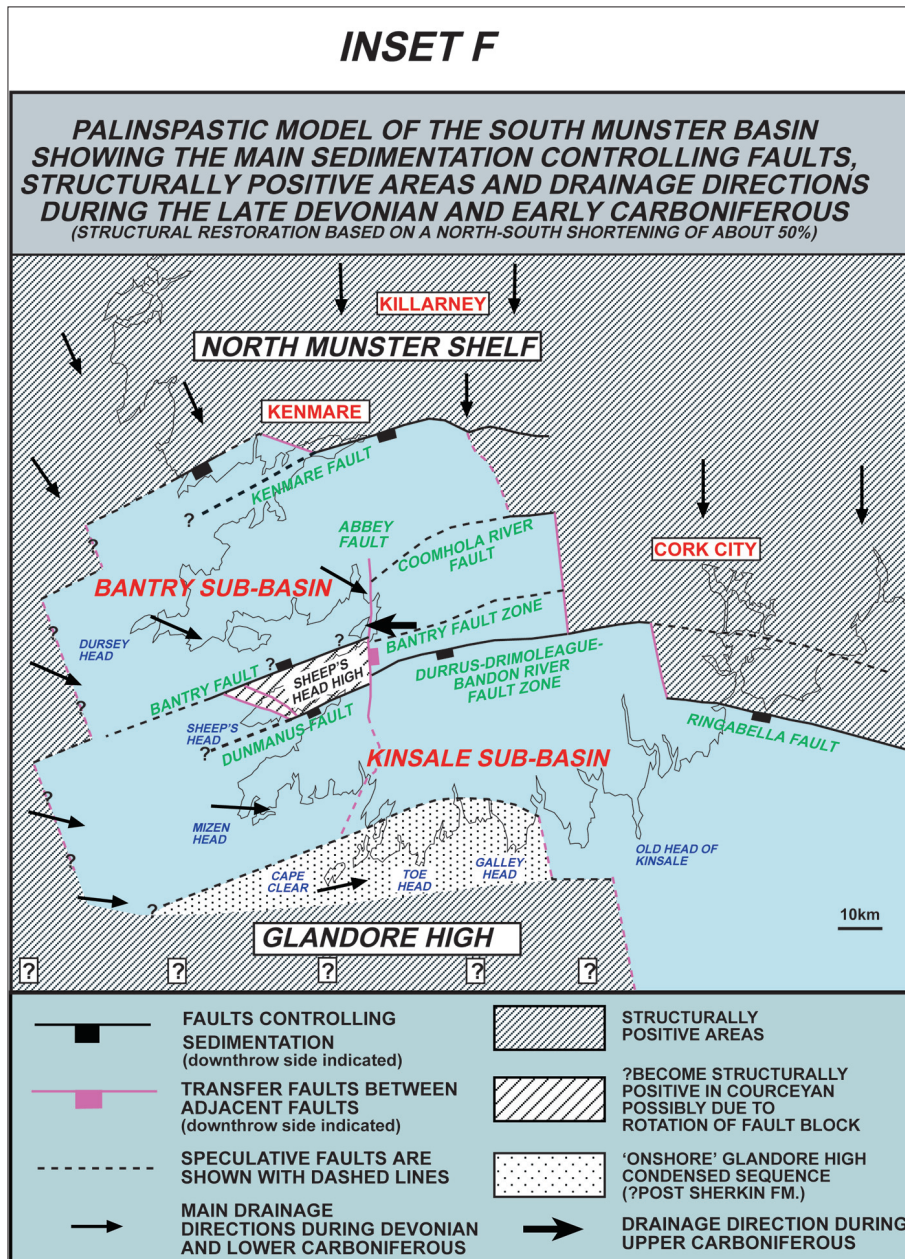
This inset map shows the outline of the Munster Basin in yellow. This was a major sedimentary basin, which was initiated in the middle of the Devonian Period or earlier, at least 380 million years ago. The basin accumulated in excess of 8km thickness of sediment. Towards the end of the Devonian, the South Munster Basin developed as a sub-basin where subsidence became greater than the area to the north known as the North Munster Shelf. Much of the sediment which infilled the basins was derived from high mountainous areas lying to the west, north and northeast.

Palinspastic model of the South Munster Basin

The inset map on the next page shows what the actual shape of the South Munster Basin might have been at the time of its infilling. Remember that the basin



infill was shortened by about 50% at the end of the Carboniferous due to tectonic forces from the south. This tectonic event resulted in a radical change in the shape of the basin. This map attempts to reconstruct its original shape by



unfolding the rock layers. It is important to note that the coastline as we see it today did not exist in the past. It is put in here for reference purposes only. Note that the reconstruction has resulted in the stretching of the coastline by 50% in a north-south direction. The map also shows a number of important faults, which are thought to have controlled the development of the basin.

Tectonic interpretation

At the lower left of the main map is an interpretation of a deep seismic survey across the Munster and South Munster Basins. The results clearly show the presence of the basin fills in yellow and the underlying “basement”. The study has modeled a buried granite body, which underlies part of the Iveragh Peninsula area. This body is probably the southwesterly extension of the Leinster Granite.

Summary map

And finally, the Summary Map is located on the lower right hand corner of the map and shows the distribution of the rock layers on the basis of their interpreted environments instead of their composition. It also depicts the major fold axes, which include anticlines and synclines.

Conclusion

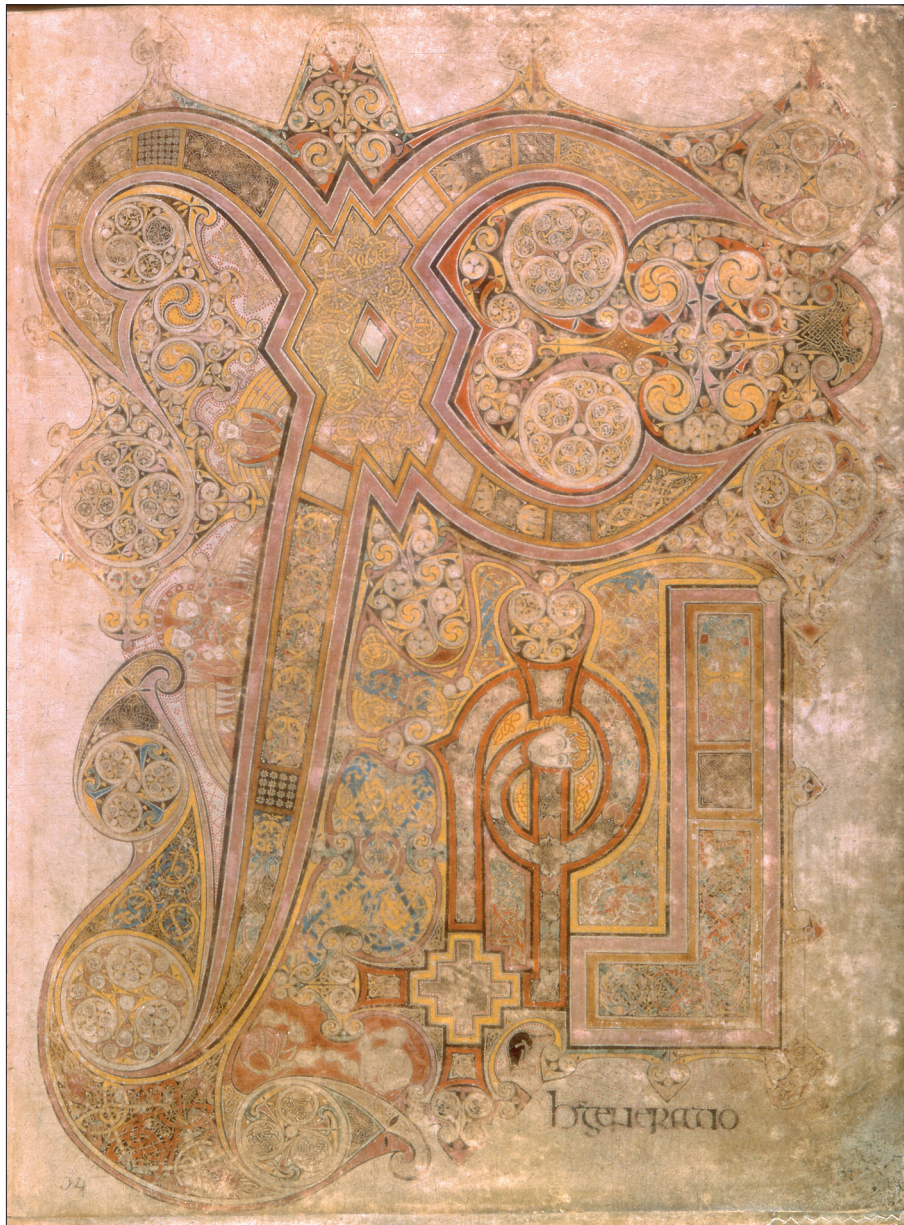
A map of this kind is like an historical manuscript. The rock layers amounting to over 8km in thickness are like the pages of the manuscript. Each layer records events and environments which existed millions of years in the past. The sequence of layers records the changing environments in the past. Once there was a sedimentary basin in this area in which sediments accumulated. They were later deformed, uplifted and fractured. They were then eroded down to the present day land surface. The map shows the outcrop of the deformed sediment layers on this surface.

The map is a model which depicts the current understanding of the history of this sedimentary basin, its structure and outcrop pattern. Further research will inevitably refine this model and through the use of new techniques will almost certainly come up with interesting new perspectives on the geology of the region.

For further reading

“New Perspectives on the Old Red Sandstone,” edited by P. F. Friend and B. P. J. Williams (London: Geological Society of London, 2000); “Sheet 24 Geology of West Cork,” by

MacCarthy, Sleeman and Pracht (Dublin: Geological Survey of Ireland, 2001); "A Geological Description of West Cork and Adjacent Parts to Accompany the Bedrock Geology 1:100,000 Scale Map Series, Sheet 24: West Cork," by Sleeman and Pracht (Dublin: Geological Survey of Ireland, 2002); and "Geology of the Devonian-Carboniferous South Munster Basin, Ireland," by MacCarthy (Cork: University College, Cork, 2004).



15

Two Pages from the *Book of Kells*

Jennifer O'Reilly

One of the principal tools of the history of art is *iconography*, the study of symbols and narratives in visual art. As a method, iconography can be demanding and exact. The art historian Erwin Panofsky pictured “iconographical analysis” as leading to a more general understanding of culture, historical processes, and “intrinsic meaning.”

This brief note gives the flavour of an iconographical analysis: it is a kind of close reading, bent on precision and thoroughness. It also hints at the wider reading of the manuscript’s significance.

Introduction

Insular gospel books, which were also precious liturgical objects, characteristically apply motifs from the traditions of Celtic and Saxon fine metalwork to the decoration of the written word, most notably in display scripts at the opening of the sacred text. In the *Book of Kells* the native repertoire of abstract ornament (curvilinear patterns of trumpets, petals and spirals; rectilinear fret and step patterns; ribbon and zoomorphic interlace; highly stylised animals) is combined with imports from the representational art of the Mediterranean world, such as vine scrolls, lions, peacocks and human figures.

Different categories of ornament, which are clearly defined and separated as if within the cell-walls of a piece of precious metalwork in other Insular gospel books, occasionally overspill their boundaries in the *Book of Kells*. The framing bands which outline the individual letter forms and delineate their panels of ornament also help unify the whole design by their color and line.

Folio 29

The first page of St Matthew’s gospel (folio 29 in the manuscript, shown on the next page) bears only two words, *Liber generationis*, yet is almost illegible. The



circular bosses, curves and spinning spirals of *Liber* are counterpoised by the rectangular multiple frames holding *generationis*. The first syllable, *Lib*, forms a sweeping ligature which spans the entire page, its last letter encircling the second syllable, *er*.



Below, the shrunken word *gene/rati/onis* is divided into three lines with letter forms of almost runic obscurity; two lines are shown in orange letters on purple and the centre line in purple on orange.

This display script, in which text dissolves and becomes image, has been described as sacred calligraphy. Discerning the form of the words, whose letters are distorted in shape and relative size and veiled by the ornament, provides some visual analogy to the monastic practice of *lectio divina* in which the reader meditatively seeks the spiritual meaning concealed beneath the literal text of the Scriptures.

Significance of the page

Matthew 1:1-17, beginning with the words *Liber generationis* (the Book of the Generation, or Genealogy), records Christ's human lineage from the royal house of Judah. The following verse begins the account of the incarnation, which stresses Christ's divine as well as his human nature. Patristic and Insular biblical commentators customarily linked the account of Christ's human birth and consequent mortality announced in Matthew 1:18 with his identification as the divine Creator at the opening of John's gospel. The text begins with Christ's name, in which commentators believed his identity was symbolically made known. It is a characteristic feature of Insular gospel books that they embellish the opening of this text to equal or even surpass the decorated opening of the gospel itself.

Folio 34

In the *Book of Kells* folio 34, shown at the beginning of this Chapter only the first three words of Matthew 1:18 are shown: *Christi autem (h) generatio*. The second and third words are written in Insular majuscule script and lie almost unnoticed at the bottom of the page (see the detail on the next page). The first word, *Christi*, is shown through the customary form XP, derived from the Greek letters *chi* and *rho*, which are the first two letters of the Greek title Christ (Messiah, "the Anointed One").

The Kells artist has transformed this ancient pictorial convention of abbreviation of the sacred name so that the initial letter embraces the whole page. The four curved arms of the *chi* radiate from a great central lozenge and terminate in spools of Celtic spirals and roundels; the much smaller letter *rho* and the Latin ending "i" stem from extensions of an equilateral cross. A foreshortened diagonal version of this golden cross appears in the rhombus or lozenge at the heart of the *chi*.





Details

The page teems with life. It is inhabited by creatures of earth, air and water: within the lozenge, an image of the quadripartite cosmos, are four tiny human figures; to the left of the *chi* are moths and angels and at the bottom of the page



are cats and mice and a black otter with a fish in its jaws. Even the interlace ornament is formed from vine scrolls and stylised birds, serpents, quadrupeds and humans.

The decoration of the text of Christ's birth suggests the identification of Christ incarnate with Christ the Creator-Logos. Christ as the divine Word is here revealed in a word, in a single letter, concealed within the design. Similarly, commentators meditating on his name at this point in Matthew's gospel, described his divinity as lying hidden in his creation, beneath his human flesh at his incarnation and beneath the literal letter of the scriptural text.

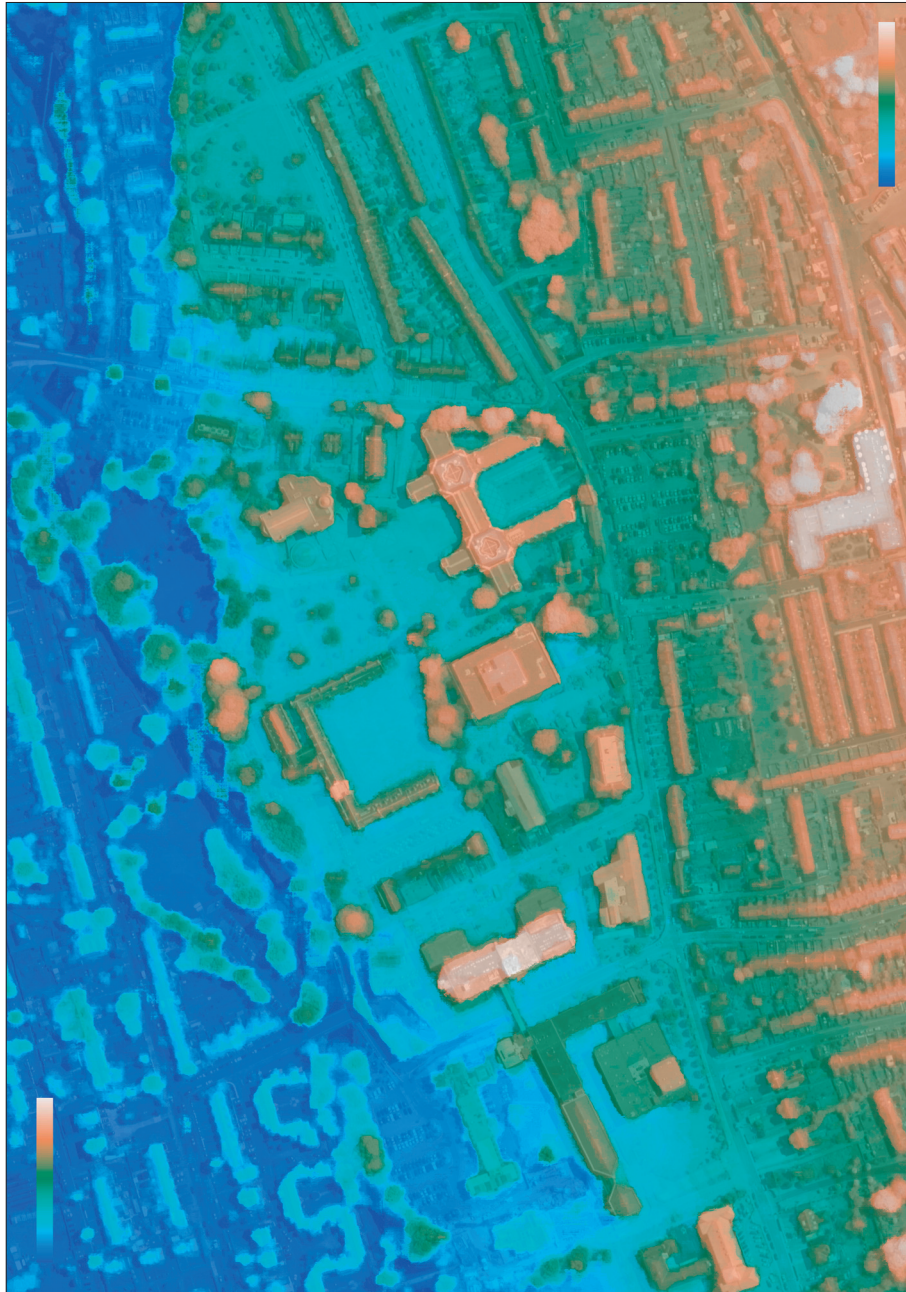
What would be next?

A student of Insular manuscripts would study a wide range of images like these, to build a sense of why they were made, how they developed, and what they signified. Images in art history are rarely studied in isolation, even though they are sometimes shown that way in galleries.

For further reading

Bernard Meehan, *An Illustrated Introduction to the Manuscript in Trinity College, Dublin* (London: Thames and Hudson, 1994); Carol Ann Farr, *The Book of Kells: Its Function and Audience* (London: British Library, 1997).





16

A High Resolution, Multichannel Aerial Photograph

Jim McGrath

This is a digital photograph of an area around the University College Cork in Ireland. The image is a composite, made up of a black and white image overlaid with a digital elevation model (DEM) that is colored, in the language of cartography, “according to an elevation look-up-table.” Two scales from the look-up table are inset to give a qualitative idea of the color range.

This is no ordinary aerial photograph, but a complicated product of multiple cameras and digital processing. It is an intriguing example of a photographic technology that produces *more information* than can be seen at any given moment.

The camera

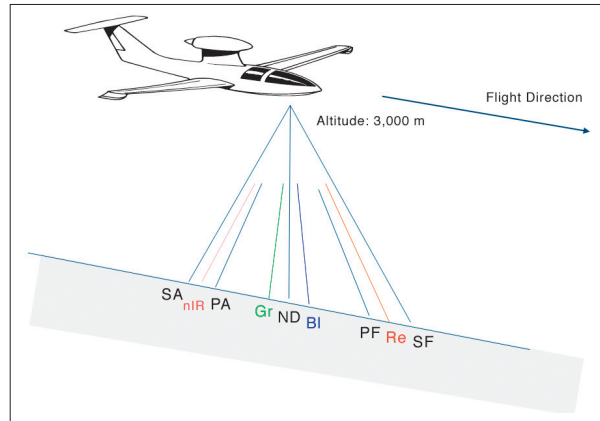
The camera used to take this image is called the High Resolution Stereo Camera-Airborne (HRSC-A). In use, the camera is mounted on the bottom of a plane.



Nine lenses

The onboard camera has nine distinct CCD (charge-coupled device) lines. Four of the lines are designed to provide multi-spectral information. To achieve this, they are each filtered differently to respond to (a) three color regions of the visible spectrum (red, green and blue) and (b) the near infrared thermal band, labelled *nIR*.

The five remaining lines (see illustrations on the next page) are configured to capture panchromatic (full-color) images at angles of +20.5°, -20.5°, +12°, -12°



and 0° respectively. Any two of these five images can subsequently be projected in red and green to produce a stereo anaglyph image (more on this later).

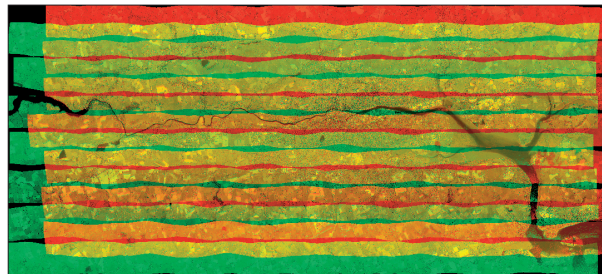
Flying over Cork, Ireland

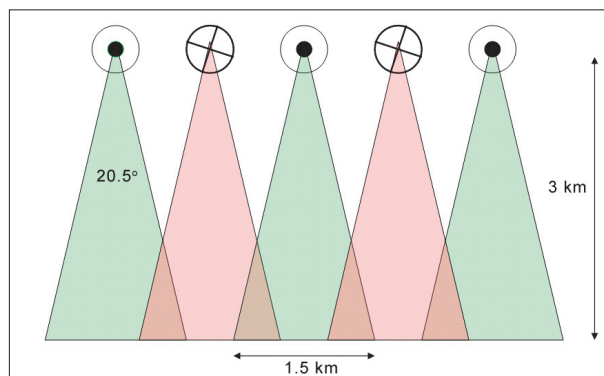
To generate the imagery, the plane flew fourteen “flight strips,” back and forth over the city (see photo below). The diagram on the next page shows the plane flying toward the viewer, and away (circles and crosses).

While traversing each of the 14 flight strips, each line of the airborne camera photographed over 100,000 “linear segments.” Each linear segment is 15 cm long (measured in the direction the plane was flying) and 12,000 pixels wide.

Registration and geo-referencing

Each flight strip was then sewn together to make a seamless mosaic, free of distortion. To do so it was necessary to take into account the triangulation of the landscape using only a few known ground control points, inverse kinematics based upon differential satellite GPS (Global Positioning System) information, and the recorded orientation (yaw, pitch, roll) of the plane.

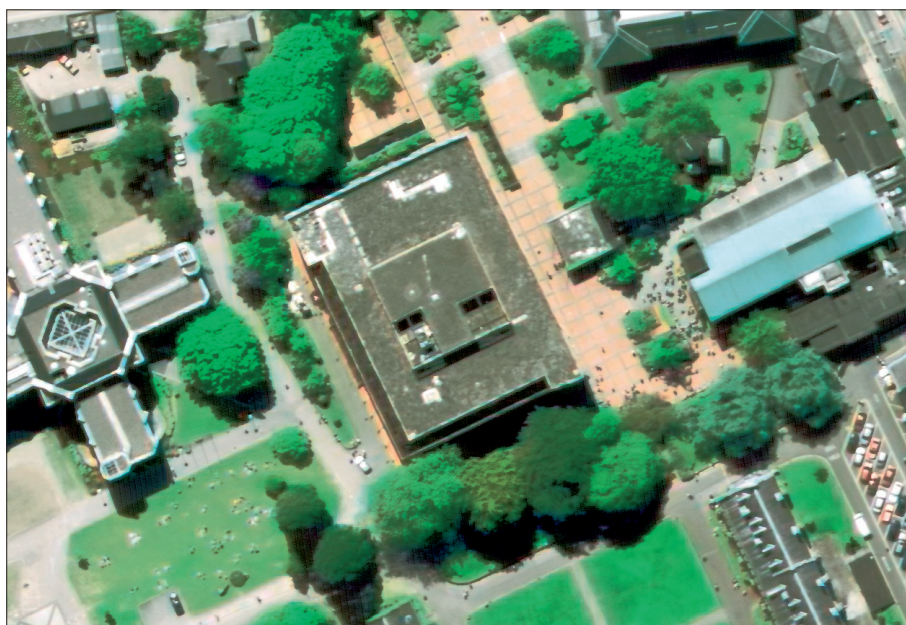




This method ensured that the various datasets were co-registered and automatically geo-referenced to the Irish National Grid. Computer software and digital processing were applied at each stage to fully automate an otherwise labor-intensive photogrammetric operation.

Resolution

The positional accuracy of data in the ortho-imagery has a maximum deviation from truth of 25 cm — very accurate given the plane's height of 3 kilometers.



The resolution of the camera itself allows a 15 cm pixel size for the Nadir Panchromatic channel and 30 cm pixel size for the other eight channels.

The photo at the bottom of the preceding page gives an indication of the minimum scale of discernable features. The university library is at the centre. Cars are clearly visible, and people are milling in front of the student café and sitting on the green in front of the humanities building.

Digital elevation model

Often images like these can be useful as-is, or they can be given false colors to bring out features of the landscape. In other cases, however, what is needed is quantitative information.

The stereo perspective viewing channels may be analysed to produce a Digital Elevation Model of the study area. The German Aerospace Agency (DLR) has provided an extremely robust, high-resolution DEM that offers a horizontal resolution of 1 meter with elevation values expressed to the nearest 10 cm.

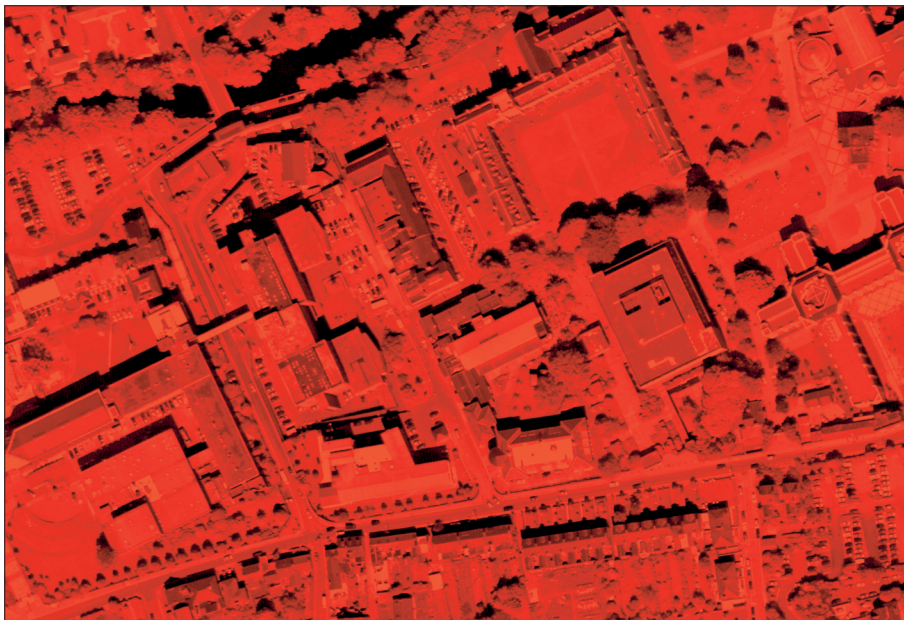
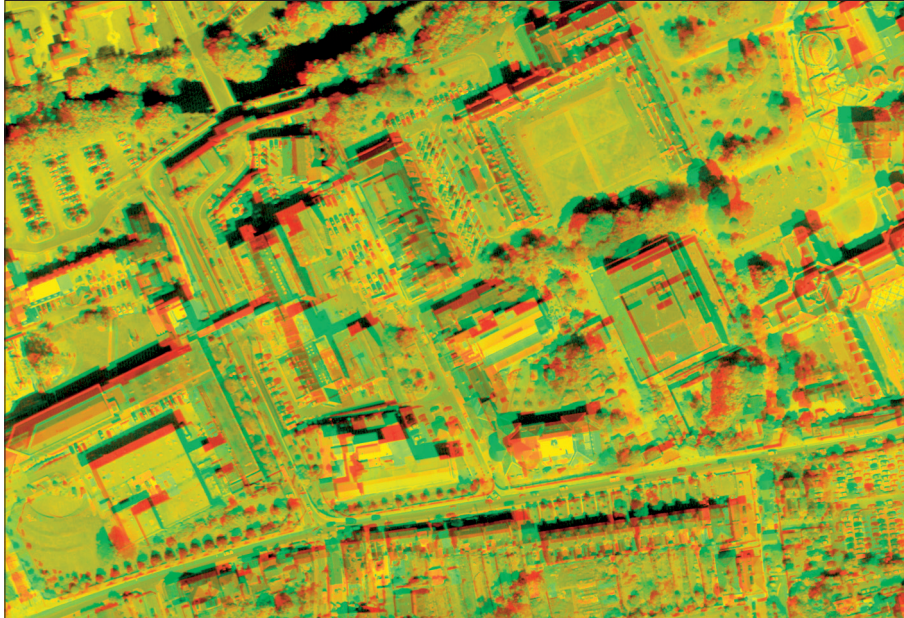
It is possible to re-analyze the stereo images to produce a DEM with different properties. Known as “stereo matching,” the method estimates depth by measuring the relative location of the same feature or pattern in two perspective images. This matching may be achieved by, for example, computing a Sum of Absolute Difference or by statistical correlation between two or more perspective images. The simpler “SAD” formula, which searches for the disparity at which the difference between two image regions is minimised, is this —

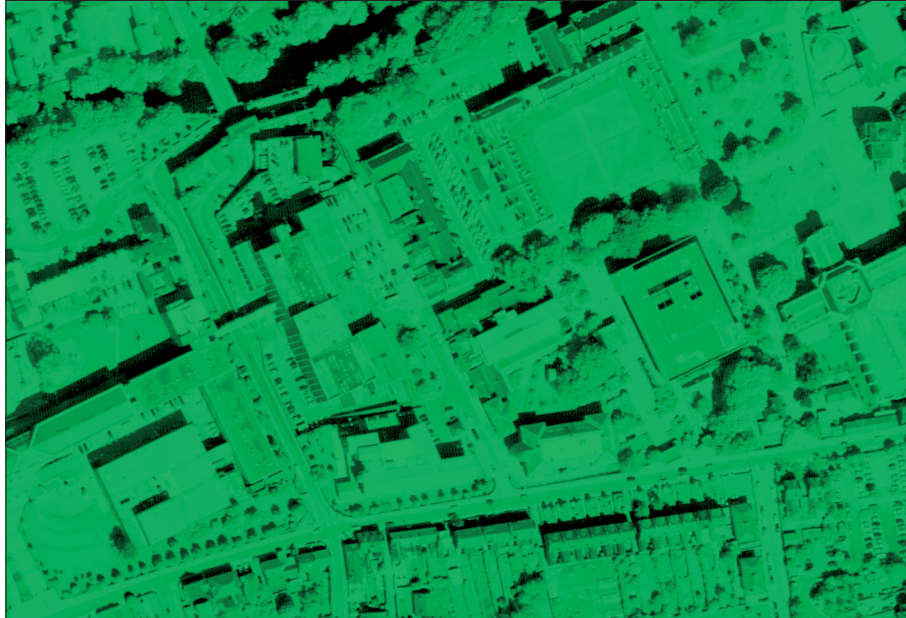
$$sad[disp] = \sum_{r=-\frac{R}{2}}^{\frac{R}{2}} \sum_{c=-\frac{C}{2}}^{\frac{C}{2}} leftimage[r][c] - rightimage[r][c + disp].$$

— where the indices (r, c) are the addresses of the pixels in each image, r is the row of the image analysis window, c is the column of the image analysis window, R is the total number of rows in the image analysis window, C is the total number of columns in the image analysis window and “ $disp$ ” is the disparity or parallax — the distance by which the analysis window has moved in the right image relative to that in the left image.

Producing a digital elevation model

Before we show the results of these analyses, here is another application of the same technology. The photo on the next page is an anaglyphic image of part of the campus of the university. An anaglyph is a stereo image printed so that one eye sees a red image, and the other a green image. (The next two photos are the constituent red and green images for the anaglyph.) If you have a pair of ana-





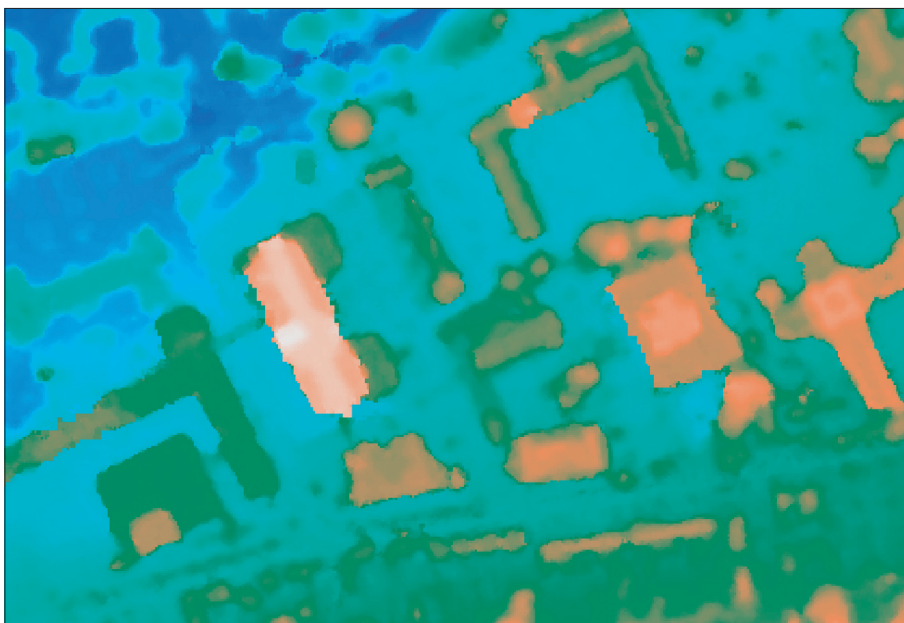
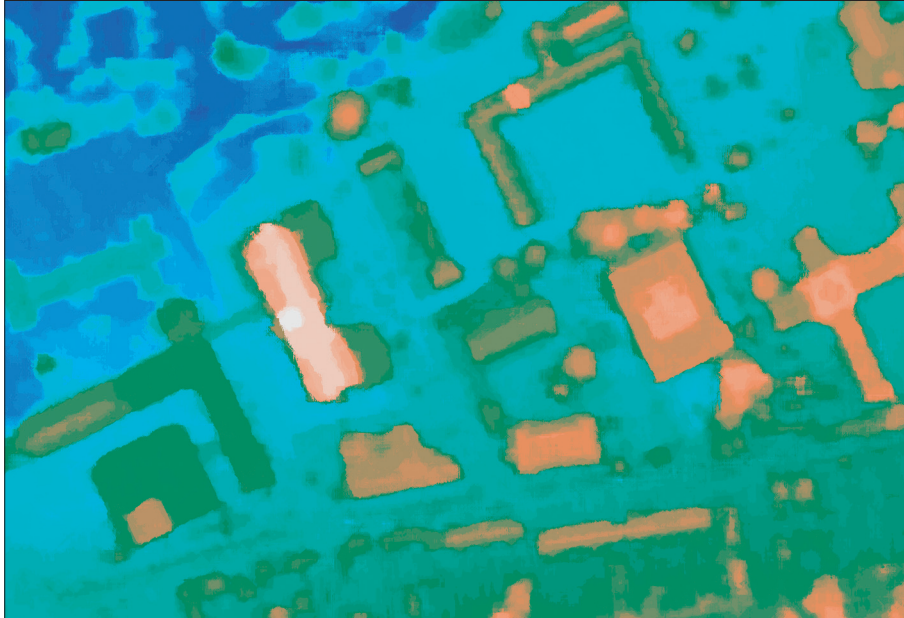
glyph-viewing glasses — one eye with a red lens, the other one blue — you should see three dimensions in the image. (Glasses can also be made with transparent sheets of colored plastic film.)

Anaglyphs have a long history, and they used to be drawn by hand before photography. Mathematicians, architects, and engineers have used them to visualize difficult structures. In 2003, the European Space Agency's Mars Express entered orbit and began sending back similar anaglyph images of the Martian surface which may be viewed on the ESA website.

Anaglyphs are more sensitive to the viewer's position than ordinary photographs. If you have anaglyphic glasses, try moving your head as you look at the image. The buildings seem to shear: an illusion based on assumptions the brain makes about the relation between your eyes and the world.

Measuring elevation

These last two pictures show the result of applying the SAD formula. They show, in close-up, the central quad of the university, with the library and student café. The idea is to tune the DEM to be sharper so that instantaneous changes in elevation are supported and the DEM's smoothing is reduced. This kind of image can be directly measured, and used to generate quantitative data.



Using the data

A project, funded by Ordnance Survey Ireland, is underway at University College Cork to analyze the aerial photography, automatically identifying features such as roads and buildings to speed-up the map-making process. It is hoped that an improved DEM will augment this analysis.

Since 1998, a number of projects at the Department of Civil and Environmental Engineering, have exploited high-resolution DEMs in the hydrodynamic and hydrological modelling of the River Lee in Cork and the River Feale in North Kerry, an adjoining county in Ireland. Reliable high-resolution DEMs may also be used to accurately measure the quantity of material extracted or deposited at quarries and landfill sites.

For more information

Follow the European Space Agency's Mars Express programme and view stunning anaglyph images of Mars taken with the HRSC camera: www.esa.int/SPECIALS/Mars_Express/

Jim McGrath, Kevin Barry, Philip O'Kane, and Richard Kavanagh, UCC, "High Resolution DEM and Sea Level Rise in the Centre of Cork-Blue City Project," Impacts of Climate Change, Urban Hydrology: Stormwater Management, National Hydrology Seminar, 11th November 2003, Tullamore Court Hotel, Ireland; Luca Migliori, J. Philip O'Kane, "The Hydrology and Hydraulics of a Pumped Polder in North Kerry – A Case Study in Hydroinformatics," Modelling of Water Quality and Quantity, The Water Framework Directive: Monitoring and Modelling Issues for River Basin Management, National Hydrology Seminar, 16th November 2004, Tullamore Court Hotel, Ireland; John Martin, "Dewatering the Lower Feale Catchment: 'A Virtual Water World,'" Ph.D. Thesis, 2002, University College, Cork, Ireland; Gerhard Neukum and the HRSC-Team, Berlin, "The HRSC-AX cameras: evaluation of the technical concept and presentation of application results after one year of operation," *Photogrammetric Week '01*, edited by D. Fritsch and R. Spiller (Heidelberg: Wichmann, 2001), 117-31; F. Wewel, F. Scholten, G. Neukum, and L. Albertz, "Digitale Luftbildaufnahme mit der HRSC — Ein Schritt in die Zukunft der Photogrammetrie," *Photogrammetrie-Fernerkundung Geoinformation*, vol. 6 (Stuttgart: E. Schweizerbart'sche Verlagsbuchhandlung, 1993), 337-48. For Viewing image processing software: www.ermapper.com.

